NUMERICAL ALGEBRA,
CONTROL AND OPTIMIZATION
Volume **6**, Number **2**, June **2016**

doi:10.3934/naco.2016008

pp. **183–219**

SINGULARLY PERTURBED DIFFUSION-ADVECTION-REACTION PROCESSES ON EXTREMELY LARGE THREE-DIMENSIONAL CURVILINEAR NETWORKS WITH A PERIODIC MICROSTRUCTURE – EFFICIENT SOLUTION STRATEGIES BASED ON HOMOGENIZATION THEORY

Erik Kropat* and Silja Meyer-Nieberg

University of the Bundeswehr Munich
Faculty of Informatics, Werner-Heisenberg-Weg 39
85577 Neubiberg, Germany

Gerhard-Wilhelm Weber+

Middle East Technical University
Institute of Applied Mathematics
06531 Ankara, Turkey

Abstract. Boundary value problems on large periodic networks arise in many applications such as soil mechanics in geophysics or the analysis of photonic crystals in nanotechnology. As a model example, singularly perturbed elliptic differential equations of second order are addressed. Typically, the length of periodicity is very small compared to the size of the covered region. The overall complexity of the networks raises serious problems on the computational side. The high density of the graph, the huge number of edges and vertices and highly oscillating coefficients necessitate solution schemes, where even a numerical approximation is no longer feasible. Realizing that such a system depends on two spatial scales - global scale (full domain) and local scale (microstructure) - a two-scale asymptotic analysis for network differential equations is applied. The limit process leads to a homogenized model on the full domain. The homogenized coefficients cover the micro-oscillations and the topology of the periodic network and characterize the effective behaviour. The approximate model's quality is guaranteed by error estimates. Furthermore, singularly perturbed microscopic models with a decreasing diffusion part and transport-dominant problems are discussed. The effectiveness of the two-scale limit analysis is demonstrated by numerical examples of diffusion-advection-reaction problems on large periodic grids.

2010 *Mathematics Subject Classification.* Primary: 4B45, 34E13, 34E05, 34E10.

Key words and phrases. Two-scale convergence asymptotic analysis, diffusion-advection-reaction equations, boundary value problems on graphs and networks, microstructures, singular perturbations.

* Corresponding author: Erik Kropat.

+ Honorary positions: Faculty of Economics, Business and Law, University of Siegen, Germany; Center for Research on Optimization and Control, University of Aveiro, Portugal; University of North Sumatra, Indonesia.

The reviewing process of the paper was handled by Herman Mawengkang as Guest Editor.

1. **Introduction.** This study is motivated by our work on OR-based models on *groundmotion prediction* [32] as well as management and monitoring of *groundwater contamination*. These applications are concerned with groundwater system optimization, the assessment of environmental risks, localization and costs of wells and pumping systems as well as cost-effective policies for remediation [9]. Generally, the flow and transport of contaminants through the soil can be determined by so-called *capillary models*. The underlying domain of such models is given by a *periodic network* that represents the *capillary system*. In our studies, we are concerned with *diffusion-advection-reaction models* that describe the distribution of certain substances like chemicals and radioactive tracers in the soil. Our experience shows that the numerical solution of the differential equations on the underlying *capillary networks* is very challenging and time-consuming.

In particular, we are interested in very large regions and comparably small periodic networks with a huge number of edges and an extremely large number of singularities - the intermediate nodes of the network. This high number of branches and the transmission conditions at the singularities of the network raise serious problems on the numerical side. Even artificial examples on very small regions cannot be solved in a reasonable time. Since the determination of the distribution of contaminants is an important part of our studies on groundwater contamination, we are interested in *approximate models*, that can be easily solved and lead to *excellent approximations of the solution of the network differential equation*.

Capillary models in geophysics, oil exploration and soil mechanics usually rely on *porous media approaches* [3, 8, 16]. The effective flow and transport through the soil are modeled by *boundary value problems on graphs* where the three-dimensional pore structure is represented by a *periodic network of capillaries*. Typically, the branches of the network have a positive thickness and the corresponding approaches can be summarized as models on *thin domains* [26, 10] and *fattened graphs* [5]. Various authors from different disciplines addressed boundary value problems on such periodic network structures. For example, diffusion/adsorption/advection macrotransport in soils are discussed by Auriault and Lewandoska [2].

A problem from geophysics is addressed in Arbogast et al., where Darcy flows in naturally fractured petroleum reservoirs are discussed [1]. Ng and Mei present a formal derivation of the macroscale effective equations of flow and chemical transport in context of ground water contamination by homogenization theory. They obtain the macroscale equations governing the convective diffusion of a volatile organic compound [30].

A natural extension of these approaches are *differential equations on one-dimensional manifolds* (see Fig. 1). The thin domain, that usually has the same spatial dimension as the overall covering domain $\Omega \subset \mathbb{R}^3$, is replaced by a network of locally one-dimensional branches. Hereby, the corresponding mathematical models have to change their type and this leads to serious problems on the mathematical side. In particular, the corresponding network model has now to include transmission conditions at the intermediate nodes. The solutions of these models have to fulfill additional continuity conditions at the ramification nodes for the solutions on the adjacent edges.

In the field of mechatronics Lenczner et al. discussed differential equations on networks in the context of cellular electronic circuits of *microelectromechanical systems* [24, 25], *smart materials* [7] and *field effect microscopy* [23]. A model for two-dimensional *resistive networks* is presented by Vogelius in [31].

Other authors focused on applications in *material sciences*. For example, the elastic response and viscoelasticity of *rubbery polymers* is discussed in [15, 28, 29]. The rubber-like material contains a micro-structure that is represented by a microsphere. A homogenization procedure is applied in order to describe the micro-to-macro transition and the three-dimensional overall response of the *polymer network*. In nanotechnology, *photonic crystals* are considered as optical analogous to semiconductors [12]. Photonic crystals can be described by large networks with a periodic microstructure at the nanoscale. The goal is here to investigate the spectral behaviour and to identify potential band gaps [17, 19, 20, 21]. Other applications include periodic networks in *filtration* [11] and *acoustics* [6].

As a model example, we consider *diffusion-advection-reaction problems* on very large networks with a *periodic microstructure* and a *very small length of periodicity*. In contrast to other approaches for fattened graphs and thin domains, the model is directly defined on the one-dimensional manifold.

The so-called *microscopic model* comprises the non-selfadjoint second order differential equations on the branches of the network, the transmission conditions in terms of Kirchhoff laws and continuity conditions at the ramification nodes and Dirichlet boundary conditions at the outer nodes of the network. The modeling of these systems on one-dimensional manifolds results in serious computational problems. In particular, the transmission conditions at the intermediate nodes have to be taken into account what is not required for thin domains and fattened graphs. In addition, a very large number of branches and singularities at the vertices has to be considered. Furthermore, the periodic microstructure leads to *highly-oscillating coefficients* and a very fine discretization is required in the numerical solution schemes. In other words, even a numerical solution can usually not be obtained with a reasonable effort and this raises the question on how such a microscopic model could be solved.

In this paper, we discuss a *two-scale limit analysis for network functions* on ε-periodic networks based on an *asymptotic expansion* of the solution of the microscopic model. The limit process leads to an approximating *macroscopic model* that can be easily solved with standard software packages. The corresponding *homogenized coefficients* of the macroscopic model provide a characterization of the global behaviour of the microscopic model.

The limit process for differential equations on one-dimensional *singularly perturbed manifolds* is more complicated than the homogenization process on *continuous domains*. Traditional averaging procedures on continuous domains as well as on thin domains usually do not require the investigation of singularities at the intermediate nodes with several adjacent branches [4]. In addition, the solution of the microscopic model on a thin domain and the solution of the macroscopic model are defined on domains with the same dimension.

An averaging procedure based on asymptotic expansions for self-adjoint operators is proposed in [27]. Other methods mainly address *fattened graphs* and *thin domains*, where the one-dimensional branches of the underlying graph are artificially extended in the global domain [5].

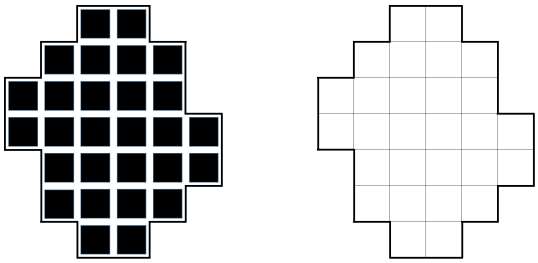

FIGURE 1. *Graph structures*: Fattened graphs (left) and one-dimensional networks (right).

In case of *microscopic models on one-dimensional manifolds*, the solution of the corresponding macroscopic model is defined on a domain in $\mathbb{R}^3$. That means, the limit process describes the convergence of a series of functions on one-dimensional manifolds to a limit function on a higher-dimensional domain. Such an averaging approach for symmetric operators was firstly discussed in [27]. Here, we further extend this approach to non-selfadjoint second-order differential equations on singularly perturbed periodic networks. We discuss the corresponding two-scale limit analysis and derive the homogenized model on the superior domain.

The so-called homogenized coefficients of the macroscopic model directly depend on the microstructure of the periodic network. In addition, we discuss the case of *singularly perturbed diffusion-advection-reaction equations*. Here, a parameter $\delta > 0$ controls the influence of the diffusion part of the microscopic model. This allows for an investigation of transport-dominant problems where the parameter δ tends to zero. Such a situation is very challenging from the numerical point of view since now *boundary-layers* occur *on each edge* of the network [14]. Fig. 2 shows the example of a transport-dominant problem on a periodic network in the plane. On each branch of the network, the solution develops a boundary layer (peak).

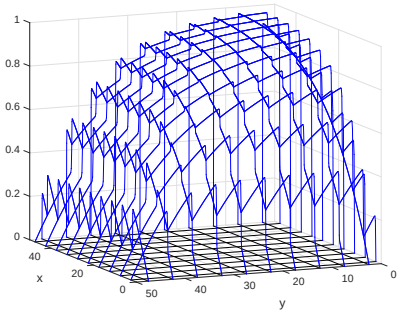

FIGURE 2. *Boundary layers*: In case of transport-dominant problems, boundary layers arise on each branch of the network.

Before we present the mathematical formulation, we shortly illustrate the averaging process at the example of a one-dimensional periodic network. The *reference graph* consists of three edges as shown in Fig. 3.

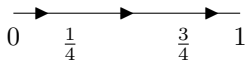

FIGURE 3. *The reference graph*: The one-dimensional network in the unit cell $[0, 1]$ consists of three edges.

The full domain is given by $\Omega = (0, 10)$ and is decomposed into a certain number of segments with three edges obtained by copying and scaling from the reference graph. The length of periodicity is given by $\varepsilon = \frac{10}{\#\text{segments}}$. The set of edges of the network $\mathcal{N}_\varepsilon^\Omega$ is given by $\mathcal{J}_\varepsilon^\Omega = \{1, \dots, 3 \cdot \#\text{segments}\}$, which is divided into three subsets $\mathcal{J}_{\varepsilon,s}^\Omega := \left\{ j = 3k - s \,\middle|\, k \in \{1, \dots, \#\text{segments}\} \right\}$ for $s = 0, 1, 2$ that correspond to the three edges of the reference graph (see Fig. 4).

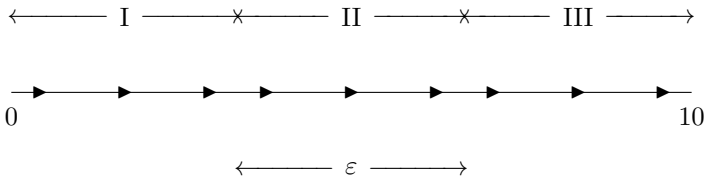

FIGURE 4. The one-dimensional network $\mathcal{N}_\varepsilon^\Omega$: Recurrent elements with three edges in the domain Ω.

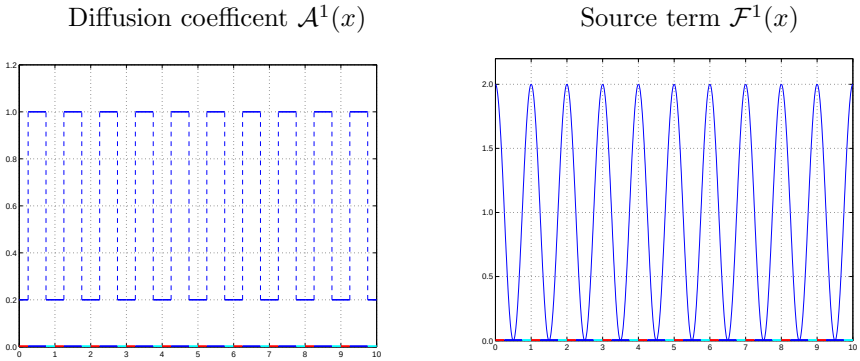

FIGURE 5. *Highly oscillating coefficients*: Diffusion coefficient and source term on the one-dimensional network $\mathcal{N}_1^\Omega$.

As an example we consider a diffusion-reaction problem on the branches of the network $\mathcal{N}_\varepsilon^\Omega$. On the branches of the reference graph, the highly oscillating diffusion coefficient is given by

$$\mathcal{A}(z) = \begin{cases} 0.2 & \text{, if } z \in \left(0, \frac{1}{4}\right), \\ 1.0 & \text{, if } z \in \left(\frac{1}{4}, \frac{3}{4}\right), \\ 0.2 & \text{, if } z \in \left(\frac{3}{4}, 1\right), \end{cases}$$

and the source term takes the form

$$\mathcal{F}(z) = 1 + \cos(2\pi \cdot z), \quad \text{if } z \in \left(0, \tfrac{1}{4}\right) \cup \left(\tfrac{1}{4}, \tfrac{3}{4}\right) \cup \left(\tfrac{3}{4}, 1\right),$$

as shown in Fig. 5. In addition, the coefficient of the reaction term is $\mathcal{D} \equiv 1$.

The microscopic model on the network $\mathcal{N}_\varepsilon^\Omega$ has the form

$$\left.\begin{aligned}
-0.2 \cdot \frac{d^2}{dl_j^2}\phi_j^\varepsilon(l_j) + \phi_j^\varepsilon(l_j) &= 1 + \cos\left(\tfrac{2\pi}{\varepsilon} \cdot l_j\right), && j \in \mathcal{J}_{\varepsilon,2}^\Omega,\ l_j \in \varepsilon\left(0, \tfrac{1}{4}\right)\\
-1.0 \cdot \frac{d^2}{dl_j^2}\phi_j^\varepsilon(l_j) + \phi_j^\varepsilon(l_j) &= 1 + \cos\left(\tfrac{2\pi}{\varepsilon} \cdot \left(l_j + \tfrac{\varepsilon}{4}\right)\right), && j \in \mathcal{J}_{\varepsilon,1}^\Omega,\ l_j \in \varepsilon\left(\tfrac{1}{4}, \tfrac{3}{4}\right)\\
-0.2 \cdot \frac{d^2}{dl_j^2}\phi_j^\varepsilon(l_j) + \phi_j^\varepsilon(l_j) &= 1 + \cos\left(\tfrac{2\pi}{\varepsilon} \cdot \left(l_j + \tfrac{3\varepsilon}{4}\right)\right), && j \in \mathcal{J}_{\varepsilon,0}^\Omega,\ l_j \in \varepsilon\left(\tfrac{3}{4}, 1\right)\\
\phi^\varepsilon(\tau) &= 0, && \text{for all boundary nodes } \tau \text{ of } \mathcal{N}_\varepsilon^\Omega,\\
\mathcal{K}_\tau^{\Omega,\varepsilon}\left(\mathcal{A}_j^\varepsilon \cdot \frac{d}{dl_j}\phi_j^\varepsilon\right) &= 0, && \text{for all ramification nodes } \tau \text{ of } \mathcal{N}_\varepsilon^\Omega,
\end{aligned}\right\} \tag{1}$$

where the *Kirchhoff functional* $\mathcal{K}_\tau^{\Omega,\varepsilon}$ determines the difference between the flow entering the ramification node τ and the flow leaving that node.

We represent the solution of the microscopic model in terms of the two-scale asymptotic expansion

$$\phi^\varepsilon(x) = \phi_0(x) + \sum_{k=1}^{\infty} \phi_k(x, z), \quad x \in \Omega,\ z \in [0, 1].$$

The application of the two-scale averaging technique discussed in this paper shows that the sequence of solutions of the microscopic model (1) converges for $\varepsilon \to 0$ towards the solution of the so-called homogenized model on the full domain Ω. The homogenized model has the form

$$\left.\begin{aligned}
-0.\overline{3} \cdot \frac{d^2}{dx^2}\phi_0(x) + \phi_0(x) &= 1, \ x \in \Omega,\\
\phi_0(x) &= 0, \ x \in \partial\Omega.
\end{aligned}\right\} \tag{2}$$

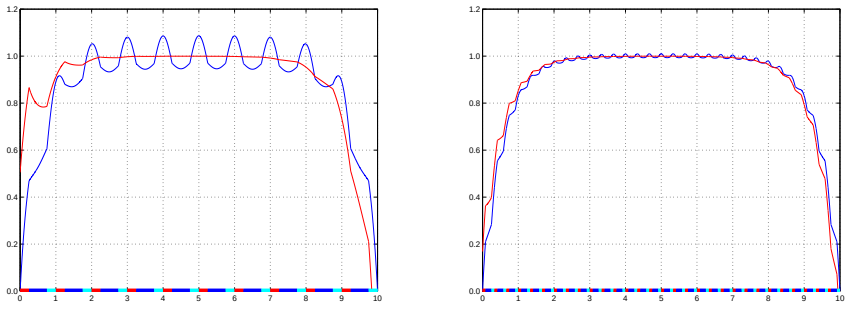

FIGURE 6. *Microscopic and macroscopic model*: The first order asymptotic expansion (red) and the exact solution (blue) of the microscopic model for $\varepsilon = 1$ (left) and $\varepsilon = \frac{1}{3}$ (right). The exact solution shows an increasing number of micro-oscillation as ε tends to zero.

Fig. 6 shows the solution of the microscopic model (blue) and the homogenized model (red) for different values of ε. The exact solution shows micro-oscillations that are caused by the periodic microstructure and the highly oscillating coefficients. As ε tends to zero, the amplitude of the micro-oscillations is decreasing. At the same time, the frequency drastically increases. This makes a numerical solution very difficult, because a very fine discretization is required to capture the effects of the micro-oscillations.

The smooth homogenized solution does not show these oscillations and provides a good approximation to the solution of the original problem for small values of ε as can be seen by Fig. 7.

The homogenized coefficients usually are not equal to the coefficients obtained by a pure averaging along the branches of the reference graph. For the diffusion coefficient in the example we obtain

$$\widehat{\mathcal{A}} = \frac{1}{\int\limits_{[0,1]} \frac{1}{\mathcal{A}(z)}\, dz} = 0.\overline{3} \neq 0.6 = \int\limits_0^1 \mathcal{A}(z)\, dz = \overline{\mathcal{A}}.$$

When we replace the homogenized boundary value problem (2) by the model

$$\left.\begin{aligned} -\overline{\mathcal{A}} \cdot \frac{d^2}{dx^2}\phi_0(x) + \phi_0(x) &= 1,\ x \in \Omega, \\ \phi_0(x) &= 0,\ x \in \partial\Omega, \end{aligned}\right\} \tag{3}$$

where $\widehat{\mathcal{A}}$ instead of the coefficient $\overline{\mathcal{A}}$ is used, we obtain the approximate "solution" that is represented by the black line in Fig. 7.

Obviously, there is great difference between the solution of (3) and the exact solution (blue) of the boundary value problem on the graph as well as the solution of the homogenized model (red).

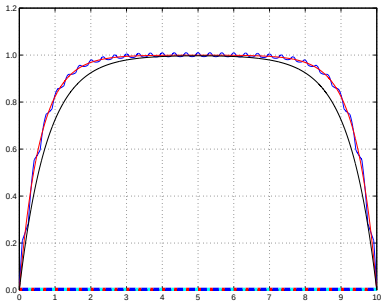

FIGURE 7. *Averaging strategies*: Exact solution of the microscopic model (blue), solution of the homogenized problem (red), and the solution obtained by traditional averaging of the coefficients (black).

The rest of the paper is organized as follows: In Section 2, some notation about *one-dimensional periodic manifolds* and the corresponding *function spaces on networks* are introduced. Section 3 discusses the *microscopic model* on the three-dimensional network. On each branch of the network, the system is defined by a diffusion-advection-reaction problem in terms of a second order differential equation. The system is singularly perturbed and the influence of the diffusion part can

be controlled by a parameter. In particular, transport-dominant problems can be considered by scaling down this parameter. Section 4 turns to *two-scale asymptotic expansions* for functions on periodic networks that are applied in the *two-scale limit analysis* in Section 5. As a result, the *approximate macroscopic model* on the full domain is derived that can be easily solved by standard software packages. The associated *homogenized coefficients* characterize the effective behaviour of the system on the full domain. Section 6 discusses so-called *regular topologies* that lead to a simplified representation of the homogenized coefficients. A *numerical example* of a diffusion-reaction problem on a three-dimensional grid is provided in Section 7. *Singularly perturbed systems* are discussed in Section 8. In particular, the influence of a vanishing diffusion part on the homogenized model is explained.

The numerical examples in Section 9 illustrate the case of *transport-dominant problems* on periodic three-dimensional grids. Finally, we conclude with a discussion of future work and potential developments of the averaging technique on one-dimensional manifolds.

2. Function Spaces on Periodic 3D-Networks.

The system under consideration is defined on the edges of a large ε-periodic network $\mathcal{N}_\varepsilon^\Omega$ (see Fig. 8). We assume that the network is contained in the domain $\Omega \subset \mathbb{R}^3$, where $\partial\Omega$ defines the outer boundary of the region of interest. Since $\mathcal{N}_\varepsilon^\Omega$ is ε-periodic, it is the restriction of an infinite ε-periodic network $\mathcal{N}_\varepsilon$ to the domain Ω, i.e., $\mathcal{N}_\varepsilon^\Omega := \mathcal{N}_\varepsilon \cap \Omega$. In addition, we assume that the total extension of the covering region Ω is considerably larger than the given length of periodicity.

Assumption 2.1. *The length of periodicity $\varepsilon > 0$ is considered as "very small" compared to the diameter of the region of interest Ω, i.e., $|\Omega| \gg \varepsilon > 0$.*

Nodes and branches

The set of nodes of the networks $\mathcal{N}_\varepsilon$ and $\mathcal{N}_\varepsilon^\Omega$ are given by $\mathcal{V}_\varepsilon$ and $\mathcal{V}\left(\mathcal{N}_\varepsilon^\Omega\right) := \mathcal{V}_\varepsilon \cap \overline{\Omega}$, respectively. The set of nodes of the restricted network $\mathcal{N}_\varepsilon^\Omega$ is composed of the *ramification nodes* $\partial^R\left(\mathcal{N}_\varepsilon^\Omega\right) := \mathcal{V}_\varepsilon \cap \Omega$ and the *boundary nodes* $\partial^B\left(\mathcal{N}_\varepsilon^\Omega\right) := \mathcal{V}_\varepsilon \cap \partial\Omega$. The restricted network $\mathcal{N}_\varepsilon^\Omega$ consists of the set of edges $\mathcal{J}_\varepsilon^\Omega$. Each branch $j \in \mathcal{J}_\varepsilon^\Omega$ is parameterized in terms of its arc length $\mathcal{L}_j^\varepsilon$ with regard to the interval $\mathcal{I}_j^\varepsilon := (0, \mathcal{L}_j^\varepsilon)$.

Unit cell and reference graph

The *unit cell* is denoted by $\square = [0,1)^3$ and $\mathcal{Z} := \mathcal{N}_1 \cap \square$ is called the *reference graph*. The networks $\mathcal{N}_\varepsilon$ and $\mathcal{N}_\varepsilon^\Omega$ are composed of recurrent elements that are obtained from the reference graph by copying and scaling with factor ε. The set of nodes of the reference graph $\mathcal{Z}$ are given by $\mathcal{V}\left(\mathcal{Z}\right) := \mathcal{V}_1 \cap \overline{\Omega}$ and they comprise the corresponding *boundary nodes* $\partial^B\left(\mathcal{Z}\right) := \mathcal{V}_1 \cap \partial\square$ and *ramification nodes* $\partial^R\left(\mathcal{Z}\right) := \mathcal{V}_1 \cap \mathrm{int}\square$. The set of edges of the reference graph is denoted $\mathcal{J}^\mathcal{Z}$ and we assume that each branch $j \in \mathcal{J}^\mathcal{Z}$ is parameterized in terms of its arc length $\mathcal{L}_j^\mathcal{Z}$ with regard to the interval $\mathcal{I}_j^\mathcal{Z} := (0, \mathcal{L}_j^\mathcal{Z})$.

3. Function Spaces on Scalable Networks.

The network differential equations are defined with regard to function spaces on one-dimensional manifolds in the d-dimensional space (here, $d = 3$). Firstly, we introduce function spaces on single branches.

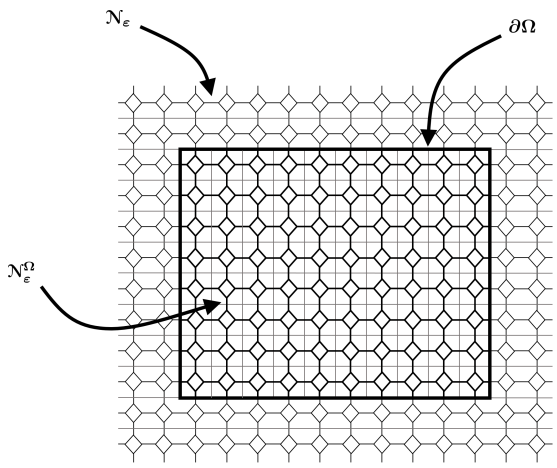

FIGURE 8. The network $\mathcal{N}_\varepsilon^\Omega$.

Definition 3.1. On each edge $j \in \mathcal{J}_\varepsilon^\Omega$ we define the Hilbert spaces

$$\mathcal{H}_\varepsilon^1\big(\mathcal{I}_j^\varepsilon\big) := \left\{ \phi_j^\varepsilon \in L^2\big(\mathcal{I}_j^\varepsilon\big) \;\middle|\; \frac{d}{dl_j}\phi_j^\varepsilon \in L^2\big(\mathcal{I}_j^\varepsilon\big) \right\},$$
$$\mathcal{H}_\varepsilon^2\big(\mathcal{I}_j^\varepsilon\big) := \left\{ \phi_j^\varepsilon \in L^2\big(\mathcal{I}_j^\varepsilon\big) \;\middle|\; \frac{d}{dl_j}\phi_j^\varepsilon \in \mathcal{H}_\varepsilon^1\big(\mathcal{I}_j^\varepsilon\big) \right\},$$

as well as the scaled norms

$$\big\|\phi_j^\varepsilon\big\|_{\mathcal{H}_\varepsilon^1(\mathcal{I}_j^\varepsilon)} := \left\{ \varepsilon^{d-1} \cdot \int\limits_{\mathcal{I}_j^\varepsilon} \left[\frac{d}{dl_j}\phi_j^\varepsilon(l_j)\right]^2 + \big[\phi_j^\varepsilon(l_j)\big]^2 \, dl_j \right\}^{\frac{1}{2}},$$

$$\big\|\phi_j^\varepsilon\big\|_{\mathcal{H}_\varepsilon^2(\mathcal{I}_j^\varepsilon)} := \left\{ \varepsilon^{d-1} \cdot \int\limits_{\mathcal{I}_j^\varepsilon} \left[\frac{d^2}{dl_j^2}\phi_j^\varepsilon(l_j)\right]^2 + \left[\frac{d}{dl_j}\phi_j^\varepsilon(l_j)\right]^2 + \big[\phi_j^\varepsilon(l_j)\big]^2 \, dl_j \right\}^{\frac{1}{2}}.$$

Then, function spaces on the network $\mathcal{N}_\varepsilon^\Omega$ can be defined.

Definition 3.2. On the ε-periodic network $\mathcal{N}_\varepsilon^\Omega$ we introduce the Hilbert space

$$\widetilde{\mathcal{H}^2}\big(\mathcal{N}_\varepsilon^\Omega\big) := \left\{ \phi^\varepsilon = \big(\phi_j^\varepsilon\big)_{j\in\mathcal{J}_\varepsilon^\Omega} \in \prod_{j\in\mathcal{J}_\varepsilon^\Omega} \mathcal{H}_\varepsilon^2\big(\mathcal{I}_j^\varepsilon\big) \;\middle|\; \sum_{j\in\mathcal{J}_\varepsilon^\Omega} \big\|\phi_j^\varepsilon\big\|^2_{\mathcal{H}_\varepsilon^2(\mathcal{I}_j^\varepsilon)} < \infty \right\}$$

with the norm

$$\big\|\phi_j^\varepsilon\big\|_{\widetilde{\mathcal{H}^2}(\mathcal{N}_\varepsilon^\Omega)} := \left\{ \sum_{j\in\mathcal{J}_\varepsilon^\Omega} \big\|\phi_j^\varepsilon\big\|^2_{\mathcal{H}_\varepsilon^2(\mathcal{I}_j^\varepsilon)} \right\}^{\frac{1}{2}}$$

and the Hilbert space

$$\mathcal{H}^2\big(\mathcal{N}_\varepsilon^\Omega\big) := \left\{ \phi^\varepsilon \in \widetilde{\mathcal{H}^2}\big(\mathcal{N}_\varepsilon^\Omega\big) \;\middle|\; \phi^\varepsilon \text{ is continuous at all } x \in \partial^R\big(\mathcal{N}_\varepsilon^\Omega\big) \right\},$$

where network functions are continuous at the ramification nodes.

4. **The Microscopic Model on the Periodic Network.** As a model problem, we consider a system of *diffusion-advection-reaction equations* on the curvilinear three-dimensional network $\mathcal{N}_\varepsilon^\Omega$. According to the structure of the network as a one-dimensional manifold the *microscopic model* consists of three parts: a) a *system of second-order differential equations* describing the behaviour of the model on each parameterized branch, b) *transmission conditions* in terms of *Kirchhoff laws* regarding the flow and *continuity conditions* that have to be fulfilled at the ramification nodes, and c) *homogeneous Dirichlet conditions* that are imposed at the outer boundary nodes of the network.

Definition 4.1. The *microscopic model* has the form

$$\left.\begin{aligned} &\text{Find } \phi^\varepsilon \in \mathcal{H}^2(\mathcal{N}_\varepsilon^\Omega) \text{ such that} \\ &\qquad \mathcal{L}_j^\varepsilon \phi_j^\varepsilon(l_j) = \mathcal{F}_j^\varepsilon(l_j),\ j \in \mathcal{J}_\varepsilon^\Omega,\ l_j \in \mathcal{I}_j^\varepsilon, \\ &\qquad\quad \phi^\varepsilon(\tau) = 0, \qquad \tau \in \partial^B\left(\mathcal{N}_\varepsilon^\Omega\right), \\ &\mathcal{K}_\tau^{\Omega,\varepsilon}\left(\mathcal{A}_j \cdot \frac{d}{dl_j}\phi_j^\varepsilon\right) = 0, \qquad \tau \in \partial^R\left(\mathcal{N}_\varepsilon^\Omega\right). \end{aligned}\right\} (\mathrm{MP}_\varepsilon)$$

System equations:

On each branch $j \in \mathcal{J}_\varepsilon^\Omega$, the second order system equation is given by

$$\begin{aligned} &\mathcal{L}_j^\varepsilon \phi_j^\varepsilon(l_j) := \\ &-\frac{d}{dl_j}\left(\delta \cdot \mathcal{A}_j\big(x(l_j), \varepsilon^{-1} l_j\big) \cdot \frac{d}{dl_j}\phi_j^\varepsilon(l_j)\right) + \frac{d}{dl_j}\left(\mathcal{B}_j\big(x(l_j), \varepsilon^{-1} l_j\big) \cdot \phi_j^\varepsilon(l_j)\right) \\ &+ \mathcal{C}_j\big(x(l_j), \varepsilon^{-1} l_j\big) \cdot \frac{d}{dl_j}\phi_j^\varepsilon(l_j) + \mathcal{D}_j\big(x(l_j), \varepsilon^{-1} l_j\big) \cdot \phi_j^\varepsilon(l_j). \end{aligned}$$

Here, $x(l_j) \in \Omega$ describes the position on the three-dimensional network in the region Ω (i.e., the *global scale*) and $z = \varepsilon^{-1} l_j \in \mathcal{Z}$ is the corresponding position on the parameterized edges of the reference graph (i.e., the *local scale*). We note that the diffusion part of the microscopic model is singularly perturbed by the parameter $\delta > 0$. This parameter regulates the influence of the diffusion part and it can be used for an investigation of transport-dominant problems where δ tends to zero. In addition, the coefficients $\mathcal{A}$, $\mathcal{B}$, $\mathcal{C}$, $\mathcal{D}$ of the system equation and the source term $\mathcal{F}$ have to fulfill the following conditions:

(C1) The coefficients $\mathcal{A}$, $\mathcal{B}$, $\mathcal{C}$, $\mathcal{D}$ and the function $\mathcal{F}$ are $\mathcal{Z} \setminus \partial^R(\mathcal{Z})$-periodic with regard to their second argument and we assume that

$$\begin{aligned} &\mathcal{A} \in C^3\big(\overline{\Omega}; \mathcal{H}^1_{per}(\mathcal{N}_1 \setminus \mathcal{V}_1)\big), \quad \mathcal{A}_{max} \geq \mathcal{A} \geq \mathcal{A}_0 > 0, \\ &\mathcal{B} \in C^3\big(\overline{\Omega}; \mathcal{H}^1_{per}(\mathcal{N}_1 \setminus \mathcal{V}_1)\big), \quad \mathcal{B}_{max} \geq \mathcal{B} \geq 0, \\ &\mathcal{C} \in C^2\big(\overline{\Omega}; \mathcal{H}^1_{per}(\mathcal{N}_1 \setminus \mathcal{V}_1)\big), \quad \mathcal{C}_{max} \geq \mathcal{C} \geq 0, \\ &\mathcal{D} \in C^1\big(\overline{\Omega}; \mathcal{H}^1_{per}(\mathcal{N}_1 \setminus \mathcal{V}_1)\big), \quad \mathcal{D}_{max} \geq \mathcal{D} \geq 0, \\ &\mathcal{F} \in C^3\big(\overline{\Omega};\, L^2_{per}(\mathcal{N}_1 \setminus \mathcal{V}_1)\big), \end{aligned}$$

where $\mathcal{H}^1_{per}(\mathcal{N}_1 \setminus \mathcal{V}_1)$ and $L^2(\mathcal{N}_1 \setminus \mathcal{V}_1)$ denote the sets of $\mathcal{Z} \setminus \partial^R(\mathcal{Z})$-periodic $\mathcal{H}^1$- or L^2-functions on the open set $\mathcal{N}_1 \setminus \mathcal{V}_1$.

(C2) For each $\tau \in \mathcal{V}_1$ we assume

$$\mathcal{K}_\tau(\mathcal{B}) = \mathcal{K}_\tau(\mathcal{C}) = 0.$$

(C3) For each branch $j \in \mathcal{J}^{\mathcal{Z}}$ and $x \in \overline{\Omega}$ we have

$$\frac{1}{2} \cdot \frac{d}{d\sigma_j} \Big(\mathcal{B}(x, \sigma_j) - \mathcal{C}(x, \sigma_j) \Big) \geq 0.$$

Transmission conditions at ramification nodes:

Since $u^\varepsilon \in \mathcal{H}^2(\mathcal{N}_\varepsilon^\Omega)$, the solution of the microscopic model fulfills *continuity conditions* at the ramification nodes of the network $\mathcal{N}_\varepsilon^\Omega$. In addition, *Kirchhoff conditions* are imposed at the ramification nodes. At each ramification node $\tau \in \partial^R \left(\mathcal{N}_\varepsilon^\Omega\right)$, the *Kirchhoff functional*

$$\mathcal{K}_\tau^{\Omega,\varepsilon}(q^\varepsilon) = \sum_{j \in \mathcal{J}_\varepsilon^{\Omega,+}(\tau)} \lim_{l_j \to \mathcal{L}_j^\varepsilon} q_j^\varepsilon(l_j) - \sum_{j \in \mathcal{J}_\varepsilon^{\Omega,-}(\tau)} \lim_{l_j \to 0} q_j^\varepsilon(l_j).$$

is defined for a given function q^ε on the network $\mathcal{N}_\varepsilon^\Omega$. Here, the index set $\mathcal{J}_\varepsilon^{\Omega,+}(\tau) \subset \mathcal{J}_\varepsilon^\Omega$ consists of all edges that terminate in the node τ and the index set $\mathcal{J}_\varepsilon^{\Omega,-}(\tau) \subset \mathcal{J}_\varepsilon^\Omega$ comprises all branches which leave the node τ. In a similar way, a Kirchhoff functional $\mathcal{K}_\tau$ can be introduced at the ramification nodes $\tau \in \mathcal{V}_\varepsilon$ of the infinite network $\mathcal{N}_\varepsilon$ and the ramification nodes $\tau \in \partial^R(\mathcal{Z})$ of the reference graph, respectively.

5. **Two-Scale Asymptotic Analysis.** In the previous section the microscopic model (MP_ε) is defined on the periodic network $\mathcal{N}_\varepsilon^\Omega$. We assume that the length of periodicity $\varepsilon > 0$ is very small compared to the diameter of the full domain $\Omega \subset \mathbb{R}^3$. This makes the numerical solution of (MP_ε) to a challenging task, because the number of vertices (i.e., the ramification nodes) and the number of edges drastically increase as ε tends to zero (what we assume here). Typically, the solution of the microscopic model requires the consideration of a large number of constraints at the ramification nodes in terms of transmission conditions and continuity conditions. In addition, each branch has to be discretized for a numerical solution and this leads to a huge algebraic system. In practice, as ε tends to zero, the number of vertices and edges can easily exceed a threshold beyond that even a numerical solution cannot be obtained in a reasonable time. The basic idea of the presented approach is to replace the complex microscopic model on the network $\mathcal{N}_\varepsilon^\Omega$ by an easy-to-solve macroscopic model on the full domain Ω that does not depend on these additional constraints. The approximating macroscopic model is derived from the microscopic model by a limit analysis where ε tends to zero.

5.1. **Two-scale asymptotic expansion.** The approximating macroscopic model is derived from the microscopic model with the help of a *two-scale asymptotic expansion*

$$u^\varepsilon(x) = u_0(x) + \sum_{k=1}^{\infty} \varepsilon^k \cdot u_k\Big(x, \frac{x}{\varepsilon}\Big). \tag{A}$$

The functions $u_k : \overline{\Omega} \times \mathcal{N}_1 \to \mathbb{R}$ are periodic with regard to their second argument.

The right-hand side of the asymptotic expansion (A) is a function of the form $u_j\big(x(l_j), \varepsilon^{-1} l_j\big)$. In this way, *two spatial length scales* are integrated in the asymptotic analysis. The first scale describes the localization within the superior domain Ω, and is also called the *slow scale*. The second scale measures the variation within the reference cell and is called the *fast scale*. In other words, the asymptotic expansion (A) reflects

(a) the *macroscopic scale*, that is described by the localization $x \in \Omega$ in the full domain, and

(b) the *microscopic scale*, that depends on the localization on the edge and the corresponding position $z = \varepsilon^{-1}x$ on the reference graph.

The asymptotic expansion (A) is now used to derive the macroscopic model and a characterization of the effective behaviour of the system on the network on a global scale. In the following subsections we show how the differential equations on each edge and the transmission conditions at the ramification nodes can be modified with regard to the asymptotic expansion (A).

5.2. **Differential equation on the edges.** In a first step, the asymptotic expansion is inserted in the differential equations on the branches of the network. For this we need the following *derivation rule* that is fulfilled on each edge j.

Theorem 5.1 (Derivation rule)**.** *Let* $\Psi \in C^1\big(\overline{\Omega}; \mathcal{H}^1_{per}(\mathcal{N}_1 \setminus \mathcal{V}_1)\big)$, $\sigma_j(l_j) := \varepsilon^{-1} l_j$ *and* $\mathcal{I}^\varepsilon_j$ *for* $j \in \mathcal{J}^\Omega_\varepsilon$, $\nabla := \left(\frac{\partial}{\partial x_1}, \ldots, \frac{\partial}{\partial x_d}\right)^T$ *denotes the gradient, "* $\circ$ *" is the scalar product in* $\mathbb{R}^d$*, and* γ_j *is a vector where the ith component is given by the cosine of the angle between the tangential direction at the branch* j *and the ith coordinate axis* [1]*. Then, the following derivation rule is fulfilled:*

$$\begin{aligned}&\frac{d}{dl_j}\Psi_j\big(x(l_j), \sigma_j(l_j)\big)\\ &= \left[\gamma_j(\sigma_j) \circ \nabla\Psi_j(x, \sigma_j) + \varepsilon^{-1} \cdot \frac{\partial}{\partial \sigma_j}\Psi_j(x, \sigma_j)\right]_{(x,\sigma_j)=(x(l_j),\sigma_j(l_j))}.\end{aligned} \tag{4}$$

Proof. Let $j \in \mathcal{J}^\Omega_\varepsilon$. Then,

$$\begin{aligned}&\frac{d}{dl_j}\Psi_j\big(x(l_j), \sigma_j(l_j)\big)\\ &= \sum_{i=1}^{d} \frac{\partial}{\partial x_i}\Psi_j\big(x(l_j), \sigma_j(l_j)\big) \cdot \frac{d}{dl_j}x_i(l_j) + \frac{\partial}{\partial \sigma_j}\Psi_j\big(x(l_j), \sigma_j(l_j)\big) \cdot \frac{d}{dl_j}\sigma_j(l_j)\\ &= \gamma_j\big(\sigma_j(l_j)\big) \circ \nabla\Psi_j\big(x(l_j), \sigma_j(l_j)\big) + \varepsilon^{-1} \cdot \frac{\partial}{\partial \sigma_j}\Psi_j\big(x(l_j), \sigma_j(l_j)\big)\\ &= \left[\gamma_j(\sigma_j) \circ \nabla\Psi_j(x, \sigma_j) + \varepsilon^{-1} \cdot \frac{\partial}{\partial \sigma_j}\Psi_j(x, \sigma_j)\right]_{(x,\sigma_j)=(x(l_j),\sigma_j(l_j))}.\end{aligned}$$

□

Now, the system equation takes the following form.

Theorem 5.2. *Let* $\Psi \in C^1\big(\overline{\Omega}; \mathcal{H}^1_{per}(\mathcal{N}_1 \setminus \mathcal{V}_1)\big)$ *and* $\sigma_j(l_j) := \varepsilon^{-1} l_j$ *and* $\mathcal{I}^\varepsilon_j$ *for* $j \in \mathcal{J}^\Omega_\varepsilon$*. Then,*

$$\begin{aligned}&\mathcal{L}^\varepsilon_j\Psi_j\big(x(l_j), \sigma_j(l_j)\big)\\ &= \left[\left(\varepsilon^{-2}\mathcal{H}_{2j} + \varepsilon^{-1}\mathcal{H}_{1j} + \mathcal{H}_{0j}\right)\Psi_j(x, \sigma_j)\right]_{(x,\sigma_j)=(x(l_j),\varepsilon^{-1}l_j)}\\ &= \Big[\mathcal{F}_j(x, \sigma_j)\Big]_{(x,\sigma_j)=(x(l_j),\varepsilon^{-1}l_j)},\end{aligned}$$

[1] See [22], page 42, for further details about the geometry.

where

$$\begin{aligned}
\mathcal{H}_{2j} &:= -\frac{\partial}{\partial\sigma_j}\Big(\delta\cdot\mathcal{A}_j(x,\sigma_j)\cdot\frac{\partial}{\partial\sigma_j}\Big),\\
\mathcal{H}_{1j} &:= -\frac{\partial}{\partial\sigma_j}\Big(\delta\cdot\mathcal{A}_j(x,\sigma_j)\cdot\gamma_j(\sigma_j)\circ\nabla\Big)-\gamma_j(\sigma_j)\circ\nabla\Big(\delta\cdot\mathcal{A}_j(x,\sigma_j)\cdot\frac{\partial}{\partial\sigma_j}\Big)\\
&\quad+\frac{\partial}{\partial\sigma_j}\mathcal{B}_j(x,\sigma_j)+\Big(\mathcal{B}_j(x,\sigma_j)+\mathcal{C}_j(x,\sigma_j)\Big)\cdot\frac{\partial}{\partial\sigma_j},\\
\mathcal{H}_{0j} &:= -\gamma_j(\sigma_j)\circ\nabla\Big(\delta\cdot\mathcal{A}_j(x,\sigma_j)\cdot\gamma_j(\sigma_j)\circ\nabla\Big)+\gamma_j(\sigma_j)\circ\nabla\mathcal{B}_j(x,\sigma_j)\\
&\quad+\Big(\mathcal{B}_j(x,\sigma_j)+\mathcal{C}_j(x,\sigma_j)\Big)\cdot\gamma_j(\sigma_j)\circ\nabla+\mathcal{D}_j(x,\sigma_j).
\end{aligned}$$

Proof. Let $j\in\mathcal{J}_\varepsilon^\Omega$. Then,

$$\begin{aligned}
&\mathcal{L}_j^\varepsilon\Psi_j\big(x(l_j),\sigma_j(l_j)\big)\\
&=-\frac{d}{dl_j}\Big(\delta\cdot\mathcal{A}_j\big(x(l_j),\varepsilon^{-1}l_j\big)\cdot\frac{d}{dl_j}\Psi_j\big(x(l_j),\varepsilon^{-1}l_j\big)\Big)\\
&\quad+\frac{d}{dl_j}\mathcal{B}_j\big(x(l_j),\varepsilon^{-1}l_j\big)\cdot\Psi_j\big(x(l_j),\varepsilon^{-1}l_j\big)\\
&\quad+\Big(\mathcal{B}_j\big(x(l_j),\varepsilon^{-1}l_j\big)+\mathcal{C}_j\big(x(l_j),\varepsilon^{-1}l_j\big)\Big)\cdot\frac{d}{dl_j}\Psi_j\big(x(l_j),\varepsilon^{-1}l_j\big)\\
&\quad+\mathcal{D}_j\big(x(l_j),\varepsilon^{-1}l_j\big)\cdot\Psi_j\big(x(l_j),\varepsilon^{-1}l_j\big)\\
&=-\Big(\gamma_j\big(\sigma_j(l_j)\big)\circ\nabla+\varepsilon^{-1}\frac{\partial}{\partial\sigma_j}\Big)\Big(\delta\cdot\mathcal{A}_j\big(x(l_j),\varepsilon^{-1}l_j\big)\cdot\Big(\gamma_j\big(\sigma_j(l_j)\big)\circ\nabla\\
&\quad+\varepsilon^{-1}\cdot\frac{\partial}{\partial\sigma_j}\Big)\Psi_j\big(x(l_j),\varepsilon^{-1}l_j\big)\Big)\\
&\quad+\Big(\Big(\gamma_j\big(\sigma_j(l_j)\big)\circ\nabla+\varepsilon^{-1}\cdot\frac{\partial}{\partial\sigma_j}\Big)\mathcal{B}_j\big(x(l_j),\varepsilon^{-1}l_j\big)\Big)\cdot\Psi_j\big(x(l_j),\varepsilon^{-1}l_j\big)\\
&\quad+\Big(\mathcal{B}_j\big(x(l_j),\varepsilon^{-1}l_j\big)+\mathcal{C}_j\big(x(l_j),\varepsilon^{-1}l_j\big)\Big)\\
&\quad\cdot\Big(\Big(\gamma_j\big(\sigma_j(l_j)\big)\circ\nabla+\varepsilon^{-1}\cdot\frac{\partial}{\partial\sigma_j}\Big)\Psi_j\big(x(l_j),\varepsilon^{-1}l_j\big)\Big)\\
&\quad+\mathcal{D}_j\big(x(l_j),\varepsilon^{-1}l_j\big)\cdot\Psi_j\big(x(l_j),\varepsilon^{-1}l_j\big)\\
&=\Big[-\gamma_j(\sigma_j)\circ\nabla\Big(\delta\cdot\mathcal{A}_j(x,\sigma_j)\cdot\gamma_j(\sigma_j)\circ\nabla\Psi_j(x,\sigma_j)\Big)\\
&\qquad+\gamma_j(\sigma_j)\circ\nabla\mathcal{B}_j(x,\sigma_j)\cdot\Psi_j(x,\sigma_j)\\
&\qquad+\Big(\mathcal{B}_j(x,\sigma_j)+\mathcal{C}_j(x,\sigma_j)\Big)\cdot\gamma_j(\sigma_j)\circ\nabla\Psi_j(x,\sigma_j)\\
&\qquad+\mathcal{D}_j(x,\sigma_j)\cdot\Psi_j(x,\sigma_j)
\end{aligned}$$

$$
\begin{aligned}
&+\varepsilon^{-1}\cdot\Big\{-\frac{\partial}{\partial\sigma_j}\Big(\delta\cdot\mathcal{A}_j(x,\sigma_j)\cdot\gamma_j(\sigma_j)\circ\nabla\Psi_j(x,\sigma_j)\Big)\\
&\qquad-\gamma_j(\sigma_j)\circ\nabla\Big(\delta\cdot\mathcal{A}_j(x,\sigma_j)\cdot\frac{\partial}{\partial\sigma_j}\Psi_j(x,\sigma_j)\Big)\\
&\qquad+\frac{\partial}{\partial\sigma_j}\mathcal{B}_j(x,\sigma_j)\cdot\Psi_j(x,\sigma_j)\\
&\qquad+\Big(\mathcal{B}_j(x,\sigma_j)+\mathcal{C}_j(x,\sigma_j)\Big)\cdot\frac{\partial}{\partial\sigma_j}\Psi_j(x,\sigma_j)\Big\}\\
&+\varepsilon^{-2}\cdot\Big\{-\frac{\partial}{\partial\sigma_j}\Big(\delta\cdot\mathcal{A}_j(x,\sigma_j)\cdot\frac{\partial}{\partial\sigma_j}\Psi_j(x,\sigma_j)\Big)\Big\}\Big]_{(x,\sigma_j)=(x(l_j),\varepsilon^{-1}l_j)}.
\end{aligned}
$$

The system equation can be represented as

$$
\begin{aligned}
\mathcal{L}_j^{\varepsilon}\Psi_j\big(x(l_j),\sigma_j(l_j)\big)&=\Big[\Big(\varepsilon^{-2}\mathcal{H}_{2j}+\varepsilon^{-1}\mathcal{H}_{1j}+\mathcal{H}_{0j}\Big)\Psi_j(x,\sigma_j)\Big]_{(x,\sigma_j)=(x(l_j),\varepsilon^{-1}l_j)}\\
&=\Big[\mathcal{F}_j(x,\sigma_j)\Big]_{(x,\sigma_j)=(x(l_j),\varepsilon^{-1}l_j)}.
\end{aligned}
$$

□

Assumption 5.3 (Scale independence)**.** *For two-scale asymptotic analysis we assume that the macroscopic scale represented by $x\in\Omega$ and the microscopic scale given by $\sigma_j\in\mathcal{I}_j^{\varepsilon}$ for each branch $j\in\mathcal{J}_{\varepsilon}^{\Omega}$ are independent.*

For the two-scale asymptotic analysis we assume later on that x and σ_j are independent. With Theorem 5.2 we obtain the following result.

Theorem 5.4. *If the scale independence from Assumption 5.3 is fulfilled, then*

$$
\Big(\varepsilon^{-2}\mathcal{H}_{2j}+\varepsilon^{-1}\mathcal{H}_{1j}+\mathcal{H}_{0j}\Big)\Psi_j(x,\sigma_j),\tag{5}
$$

where x plays the role of a parameter.

5.3. **Transmission conditions at ramification nodes.** In a second step, the Kirchhoff-operator $\mathcal{K}_\tau$ is applied to a function of the form $\Psi_j\big(x(l_j),\varepsilon^{-1}l_j\big)$.

Theorem 5.5. *Let $\Psi\in C^1\big(\overline{\Omega};\mathcal{H}^1_{per}(\mathcal{N}_1\setminus\mathcal{V}_1)\big)$ and τ is a ramification node. If the scale independence from Assumption 5.3 is fulfilled, then the following equation is fulfilled:*

$$
\mathcal{K}_0^{(\tau)}\left(\Psi_j\right)+\varepsilon^{-1}\cdot\mathcal{K}_1^{(\tau)}\left(\Psi_j\right)=0,\tag{6}
$$

where

$$
\mathcal{K}_0^{(\tau)}\left(\Psi_j\right):=\mathcal{K}_\tau\Big(\delta\cdot\mathcal{A}_j\cdot\gamma_j\circ\nabla\Psi_j\Big),\ \mathcal{K}_1^{(\tau)}\left(\Psi_j\right):=\mathcal{K}_\tau\Big(\delta\cdot\mathcal{A}_j\cdot\frac{\partial}{\partial\sigma_j}\Psi_j\Big),
$$

and x plays the role of a parameter.

Proof. With the derivation rule from Theorem 4 we obtain

$$\begin{aligned} &\mathcal{K}_\tau\left(\delta\cdot\mathcal{A}_j\cdot\frac{d}{dl_j}\Psi_j\right)=0\\ \Leftrightarrow\quad &\mathcal{K}_\tau\left(\delta\cdot\mathcal{A}_j\cdot\gamma_j\circ\nabla\Psi_j\right)+\varepsilon^{-1}\cdot\mathcal{K}_\tau\left(\delta\cdot\mathcal{A}_j\cdot\frac{\partial}{\partial\sigma_j}\Psi_j\right)=0 \end{aligned} \tag{7}$$

and

$$\mathcal{K}_0^{(\tau)}\left(\Psi_j\right)+\varepsilon^{-1}\cdot\mathcal{K}_1^{(\tau)}\left(\Psi_j\right)=0.$$

□

5.4. **Identification of the functions ϕ_k.** The functions ϕ_k, $k\in\mathbb{N}_0$, of the asymptotic expansion (A) can be identified as the solutions of *auxiliary boundary problems* on the reference graph.

Theorem 5.6. *The functions ϕ_k, $k\in\mathbb{N}_0$, of the asymptotic expansion (A) are the solutions of the following cell problems:*

$$\left.\begin{aligned} &\mathcal{H}_{2j}\phi_{1j} &&=-\mathcal{H}_{1j}\phi_0,\quad j\in\mathcal{J}_{\mathcal{Z}},\\ &\mathcal{K}_1^{(\tau)}(\phi_1) &&=-\mathcal{K}_0^{(\tau)}(\phi_0),\ \tau\in\partial^I\left(\mathcal{Z}\right),\\ &\phi_1 \textit{ is } \mathcal{Z}\textit{-periodic},\end{aligned}\right\}\ \text{(S1)}$$

and

$$\left.\begin{aligned} &\mathcal{H}_{2j}\phi_{2j} &&=-\mathcal{H}_{1j}\phi_{1j}-\mathcal{H}_{0j}\phi_0+\mathcal{F}_j,\ j\in\mathcal{J}_{\mathcal{Z}},\\ &\mathcal{K}_1^{(\tau)}(\phi_2) &&=-\mathcal{K}_0^{(\tau)}(\phi_1),\ \tau\in\partial^I\left(\mathcal{Z}\right),\\ &\phi_2 \textit{ is } \mathcal{Z}\textit{-periodic},\end{aligned}\right\}\ \text{(S2)}$$

and

$$\left.\begin{aligned} &\mathcal{H}_{2j}\phi_{kj} &&=-\mathcal{H}_{1j}\phi_{k-1j}-\mathcal{H}_{0j}\phi_{k-2j},\ j\in\mathcal{J}_{\mathcal{Z}},\\ &\mathcal{K}_1^{(\tau)}(\phi_k) &&=-\mathcal{K}_0^{(\tau)}(\phi_k),\ \tau\in\partial^I\left(\mathcal{Z}\right),\\ &\phi_k \textit{ is } \mathcal{Z}\textit{-periodic},\end{aligned}\right\}\ \text{(S3)}$$

for $k>2$.

Proof. We apply the asymptotic expansion (A) in Equation (5) to derive the form of the functions ϕ_k, $k\in\mathbb{N}_0$. With

$$\left(\varepsilon^{-2}\mathcal{H}_{2j}+\varepsilon^{-1}\mathcal{H}_{1j}+\mathcal{H}_{0j}\right)\left(\phi_0+\varepsilon\phi_{1j}+\varepsilon^2\phi_{2j}+\ldots\right)=\mathcal{F}_j,$$

we obtain the equation

$$\begin{aligned} \varepsilon^{-2}\cdot\mathcal{H}_{2j}\phi_0+\varepsilon^{-1}\cdot\mathcal{H}_{1j}\phi_0\ &+\mathcal{H}_{0j}\phi_0\\ +\varepsilon^{-1}\cdot\mathcal{H}_{2j}\phi_{1j}+\mathcal{H}_{1j}\phi_{1j}&+\varepsilon\cdot\mathcal{H}_{0j}\phi_{1j}\\ +\mathcal{H}_{2j}\phi_{2j}+\varepsilon\cdot\mathcal{H}_{1j}\phi_{2j}&+\varepsilon^2\cdot\mathcal{H}_{0j}\phi_{2j}\\ -\mathcal{F}_j\qquad&+\ldots\\ &=0 \end{aligned}$$

that is ordered by the coefficients with the same exponents of the parameter ε. The coefficient of ε^{-2} is equal to zero, because ϕ_0 does not depend on σ_j. Comparing the coefficients at the same exponents of ε leads to the following system of equations for ϕ_k:

$$\begin{aligned}
\mathcal{H}_{2j}\phi_0 &= 0,\\
\mathcal{H}_{2j}\phi_{1j} &= -\mathcal{H}_{1j}\phi_0,\\
\mathcal{H}_{2j}\phi_{2j} &= -\mathcal{H}_{1j}\phi_{1j} - \mathcal{H}_{0j}\phi_0 + \mathcal{F}_j,\\
\mathcal{H}_{2j}\phi_{kj} &= -\mathcal{H}_{1j}\phi_{k-1j} - \mathcal{H}_{0j}\phi_{k-2j}\ ,\ k>2.
\end{aligned}$$

Similarly, the asymptotic expansion (A) can be applied to the transmission conditions at the ramification nodes τ given by Equation (6). It follows

$$\mathcal{K}_0^{(\tau)}\big(\phi_0 + \varepsilon\phi_1 + \varepsilon^2\phi_2 + \ldots\big) + \varepsilon^{-1}\cdot\mathcal{K}_1^{(\tau)}\big(\phi_0 + \varepsilon\phi_1 + \varepsilon^2\phi_2 + \ldots\big) = 0,$$

and

$$\begin{aligned}
&\mathcal{K}_0^{(\tau)}(\phi_0) + \varepsilon\cdot\mathcal{K}_0^{(\tau)}(\phi_1) + \varepsilon^2\cdot\mathcal{K}_0^{(\tau)}(\phi_2) + \ldots\\
&+\varepsilon^{-1}\cdot\mathcal{K}_1^{(\tau)}(\phi_0) + \mathcal{K}_1^{(\tau)}(\phi_1) + \varepsilon\cdot\mathcal{K}_1^{(\tau)}(\phi_2) + \varepsilon^2\cdot\mathcal{K}_1^{(\tau)}(\phi_3) + \ldots = 0.
\end{aligned}$$

Comparing the coefficients at the same exponents of ε we obtain:

$$\begin{aligned}
\mathcal{K}_1^{(\tau)}(\phi_0) &= 0,\\
\mathcal{K}_1^{(\tau)}(\phi_1) &= -\mathcal{K}_0^{(\tau)}(\phi_0),\\
\mathcal{K}_1^{(\tau)}(\phi_2) &= -\mathcal{K}_0^{(\tau)}(\phi_1)\\
\mathcal{K}_1^{(\tau)}(\phi_k) &= -\mathcal{K}_0^{(\tau)}(\phi_{k-1}), \quad k>2.
\end{aligned}$$

The combination of the equations obtained for the differential equations on the branches of the network and the transmission conditions at the ramification nodes lead to the system of auxiliary boundary value problems for the functions ϕ_k. □

For the derivation of the macroscopic model the function ϕ_1 is represented in terms of the function ϕ_0.

Definition 5.7. The function ϕ_1 in the asymptotic expansion (A) is called **$\boldsymbol{\phi_0}$-representable**, if there exists a $\mathcal{Z}$-periodic vector function $\mathcal{S}:\overline{\Omega}\times\mathcal{N}_1\to\mathbb{R}^d$ that is composed of functions $\mathcal{S}^{(k)}:\overline{\Omega}\times\mathcal{N}_1\to\mathbb{R}$ with $k\in\{1,\ldots,d\}$ and a $\mathcal{Z}$-periodic function $\mathcal{T}:\overline{\Omega}\times\mathcal{N}_1\to\mathbb{R}$ such that

$$\phi_1 = \mathcal{S}\circ\nabla\phi_0 - \mathcal{T}\cdot\phi_0. \tag{8}$$

Inserting (8) in systems (S1) and (S2) we can immediately see that ϕ_1 is ϕ_0-representable.

Theorem 5.8. *The function ϕ_1 in the asymptotic expansion (A) is ϕ_0-representable. The functions $\mathcal{S}^{(k)}$ are the solutions of the systems*

$$\left.\begin{aligned} &-\frac{\partial}{\partial\sigma_j}\left(\delta\cdot a_j(x,\sigma_j)\cdot\frac{\partial}{\partial\sigma_j}\mathcal{S}_j^{(k)}(x,\sigma_j)\right)\\ &=\frac{\partial}{\partial\sigma_j}\left(\delta\cdot\mathcal{A}_j(x,\sigma_j)\cdot\gamma_j^{(k)}(\sigma_j)\right),\ j\in\mathcal{J}_{\mathcal{Z}},\\ &\mathcal{K}_1^{(\tau)}\big(\mathcal{S}^{(k)}\big)=-\mathcal{K}_0^{(\tau)}\big((x)_k\big),\ \tau\in\partial^I(\mathcal{Z}),\\ &\mathcal{S}^{(k)}\ \textit{is}\ \mathcal{Z}\textit{-periodic},\end{aligned}\right\}\text{(S4)}$$

where $(x)_k$ denotes the k-th component of the vector x, and the function $\mathcal{T}$ is the solution of the system

$$\left.\begin{aligned} &-\frac{\partial}{\partial\sigma_j}\left(\delta\cdot\mathcal{A}_j(x,\sigma_j)\cdot\frac{\partial}{\partial\sigma_j}\mathcal{T}_j(x,\sigma_j)\right)\\ &=\frac{\partial}{\partial\sigma_j}\mathcal{B}_j(x,\sigma_j),\ j\in\mathcal{J}_{\mathcal{Z}},\\ &\mathcal{K}_1^{(\tau)}\big(\mathcal{T}\big)=0,\ \tau\in\partial^I(\mathcal{Z}),\\ &\mathcal{T}\ \textit{is}\ \mathcal{Z}\textit{-periodic}.\end{aligned}\right\}\text{(S5)}$$

The solvability of the systems (S1)-(S5) is guaranteed by the following lemma[2].

Lemma 5.9. *Let $k\in\mathbb{N}_0$ and $\mathcal{F}\in C^k\big(\overline{\Omega};L^2(\mathcal{Z})\big)$ be $\mathcal{Z}$-periodic. The problem*

$$\left.\begin{aligned} -\frac{\partial}{\partial\sigma_j}\left(\mathcal{A}_j(x,\sigma_j)\cdot\frac{\partial}{\partial\sigma_j}\Psi_j(x,\sigma_j)\right)&=\mathcal{F}_j\,(x,\sigma_j)\,,\ j\in\mathcal{J}_{\mathcal{Z}},\\ -\mathcal{K}_1^{(\tau)}\,(\Psi)&=\mathcal{G}_\tau\,(x)\,,\ \tau\in\partial^I(\mathcal{Z}),\end{aligned}\right\}\text{(CP)}$$

has a solution in $C^k\big(\overline{\Omega};H^1_{per}\big)$, if the following condition is fulfilled:

$$\sum_{j\in\mathcal{J}_{\mathcal{Z}}}\int_{\mathcal{J}_j^{\mathcal{Z}}}\mathcal{F}_j\,(x,\sigma_j)\,d\sigma_j=\sum_{\tau\in\partial^R(\mathcal{Z})}\mathcal{G}_\tau(x).\qquad\text{(C)}$$

Remark 1. Each solution of (CP) is defined up to an additive constant. Here, we define that the unique solution of (CP) has to fulfill the following condition:

$$\sum_{j\in\mathcal{J}_{\mathcal{Z}}}\int_{\mathcal{J}_j^{\mathcal{Z}}}\Psi_j\,(x,\sigma_j)\,d\sigma_j=0.$$

[2]See also lemma 19.2.1, p. 260, in [27].

6. **Macroscopic Model.** In this section, the homogenized counterpart to the microscopic model is derived. The *homogenized coefficients* of the so-called *macroscopic model* characterize the behaviour of the microscopic model on the network on a global scale. For the limit analysis it is not necessary to rely on the full asymptotic expansion (A). It is sufficient to focus on the *first-order asymptotic expansion* $\phi^\varepsilon = \phi_0 + \varepsilon\phi_1$ and the system (S2). The following theorem introduces the macroscopic model.

Theorem 6.1. *The function $\phi_0 : \Omega \to \mathbb{R}$ is the solution of the following macroscopic model*

$$\left.\begin{aligned} \mathcal{L}^0\phi_0(x) &= \widehat{\mathcal{F}}(x), \quad x \in \Omega, \\ \phi_0(x) &= 0 \qquad , \quad x \in \partial\Omega. \end{aligned}\right\} (\mathrm{MP}_0)$$

Here, $\mathcal{L}^0$ is defined by

$$\begin{aligned} \mathcal{L}^0\phi_0(x) := &- \sum_{s,k=1}^{d} \frac{\partial}{\partial x_s}\left(\widehat{\mathcal{A}}_{sk}(x)\cdot\frac{\partial}{\partial x_k}\phi_0(x)\right) + \sum_{k=1}^{d}\frac{\partial}{\partial x_k}\left(\widehat{\mathcal{B}}_k(x)\cdot\phi_0(x)\right) \\ &+ \sum_{k=1}^{3}\widehat{\mathcal{C}}_k(x)\cdot\frac{\partial}{\partial x_k}\phi_0(x) + \widehat{\mathcal{D}}(x)\cdot\phi_0(x) \end{aligned}$$

and the homogenized coefficients of the macroscopic model are given by

$$\widehat{\mathcal{A}}_{sk}(x) = \sum_{j\in\mathcal{J}_z}\int_{\mathcal{Y}_j^z} \delta\cdot\mathcal{A}_j(x,\sigma_j)\cdot\gamma_j^{(s)}(\sigma_j)\left(\gamma_j^{(k)}(\sigma_j) + \frac{\partial}{\partial\sigma_j}\mathcal{S}_j^{(k)}(x,\sigma_j)\right)d\sigma_j,$$

$$\widehat{\mathcal{B}}_k(x) = \sum_{j\in\mathcal{J}_z}\int_{\mathcal{Y}_j^z} \gamma_j^{(k)}(\sigma_j)\left(\mathcal{B}_j(x,\sigma_j) + \delta\cdot\mathcal{A}_j(x,\sigma_j)\cdot\frac{\partial}{\partial\sigma_j}\mathcal{T}_j(x,\sigma_j)\right)d\sigma_j,$$

$$\begin{aligned} \widehat{\mathcal{C}}_k(x) = \sum_{j\in\mathcal{J}_z}\int_{\mathcal{Y}_j^z} &\mathcal{C}_j(x,\sigma_j)\left(\gamma_j^{(k)}(\sigma_j) + \frac{\partial}{\partial\sigma_j}\mathcal{S}_j^{(k)}(x,\sigma_j)\right) \\ &+ \frac{\partial}{\partial\sigma_j}\left(\mathcal{B}_j(x,\sigma_j)\cdot\mathcal{S}_j^{(k)}(x,\sigma_j)\right)d\sigma_j, \end{aligned}$$

$$\begin{aligned} \widehat{\mathcal{D}}(x) = \sum_{j\in\mathcal{J}_z}\int_{\mathcal{Y}_j^z} &\mathcal{D}_j(x,\sigma_j) - \mathcal{C}_j(x,\sigma_j)\cdot\frac{\partial}{\partial\sigma_j}\mathcal{T}_j(x,\sigma_j) \\ &- \frac{\partial}{\partial\sigma_j}\left(\mathcal{B}_j(x,\sigma_j)\cdot\mathcal{T}_j(x,\sigma_j)\right)d\sigma_j, \end{aligned}$$

$$\widehat{\mathcal{F}}(x) = \sum_{j\in\mathcal{J}_z}\int_{\mathcal{Y}_j^z}\mathcal{F}_j(x,\sigma_j)\,d\sigma_j.$$

Proof. The coefficient ϕ_2 of the asymptotic expansion (A) is the solution of system (S2). The first equation of (S2) is given by

$$\mathcal{H}_{2j}\phi_{2j}(x,\sigma_j) = -\mathcal{H}_{1j}\phi_{1j}(x,\sigma_j) - \mathcal{H}_{0j}\phi_0(x) + \mathcal{F}_j(x,\sigma_j).$$

In order to prove the condition (C), the right hand side of this equation has to be integrated on all edges of the reference graph. With the second equation of system (S2) we have to show that

$$\begin{aligned}
&\sum_{j\in\mathcal{J}_z}\int_{\mathcal{I}_j^z}\frac{\partial}{\partial\sigma_j}\Big(\delta\cdot\mathcal{A}_j(x,\sigma_j)\cdot\gamma_j(\lambda_j)*\nabla\phi_{1j}(x,\sigma_j)\Big)\,d\sigma_j\\
&+\sum_{j\in\mathcal{J}_z}\int_{\mathcal{I}_j^z}\gamma_j(\sigma_j)*\nabla\Big(\delta\cdot\mathcal{A}_j(x,\sigma_j)\cdot\frac{\partial}{\partial\sigma_j}\phi_{1j}(x,\sigma_j)\Big)\,d\sigma_j\\
&-\sum_{j\in\mathcal{J}_z}\int_{\mathcal{I}_j^z}\frac{\partial}{\partial\sigma_j}\mathcal{B}_j(x,\sigma_j)\cdot\phi_{1j}(x,\sigma_j)\,d\sigma_j\\
&-\sum_{j\in\mathcal{J}_z}\int_{\mathcal{I}_j^z}\Big(\mathcal{B}_j(x,\sigma_j)+\mathcal{C}_j(x,\sigma_j)\Big)\cdot\frac{\partial}{\partial\sigma_j}u_{1j}(x,\sigma_j)\,d\sigma_j\\
&+\sum_{j\in\mathcal{J}_z}\int_{\mathcal{I}_j^z}\gamma_j(\sigma_j)*\nabla\Big(\delta\cdot\mathcal{A}_j(x,\sigma_j)\cdot\gamma_j(\sigma_j)*\nabla\phi_0(x)\Big)\,d\sigma_j\\
&-\sum_{j\in\mathcal{J}_z}\int_{\mathcal{I}_j^z}\gamma_j(\sigma_j)*\nabla\mathcal{B}_j(x,\sigma_j)\cdot\phi_0(x)\,d\sigma_j\\
&-\sum_{j\in\mathcal{J}_z}\int_{\mathcal{I}_j^z}\Big(\mathcal{B}_j(x,\sigma_j)+\mathcal{C}_j(x,\sigma_j)\Big)\cdot\gamma_j(\sigma_j)*\nabla\phi_0(x)\,d\sigma_j\\
&-\sum_{j\in\mathcal{J}_z}\int_{\mathcal{I}_j^z}\mathcal{D}_j(x,\sigma_j)\cdot\phi_0(x)\,d\sigma_j+\mathcal{F}_j(x,\sigma_j)\,d\sigma_j=\sum_{j\in\mathcal{J}_z}\int_{\mathcal{I}_j^z}\mathcal{K}_0^{(\tau)}(\phi_1).
\end{aligned}\tag{9}$$

The first term of (9) can be represented by

$$\begin{aligned}
&\sum_{j\in\mathcal{J}_z}\int_{\mathcal{I}_j^z}\frac{\partial}{\partial\sigma_j}\Big(\delta\cdot\mathcal{A}_j(x,\sigma_j)\cdot\gamma_j(\lambda_j)*\nabla\phi_{1j}(x,\lambda_j)\Big)\,d\sigma_j\\
&=\sum_{j\in\mathcal{J}_z}\int_{\mathcal{I}_j^z}\Big[\delta\cdot\mathcal{A}_j(x,\sigma_j)\cdot\gamma_j(\lambda_j)*\nabla\phi_{1j}(x,\lambda_j)\Big]_0^{\mathcal{L}_j^z}\\
&=\sum_{\tau\in\partial^I\mathcal{Z}}\mathcal{K}_\tau\Big(\delta\cdot\mathcal{A}_j\cdot\gamma_j*\nabla\phi_{1j}\Big)=\sum_{\tau\in\partial^I\mathcal{Z}}\mathcal{K}_0^{(\tau)}(\phi_1),
\end{aligned}$$

and condition (C) is fullfilled if and only if

$$
\begin{aligned}
&- \sum_{j\in\mathcal{J}_z} \int_{\mathcal{J}_j^z} \gamma_j(\sigma_j) * \nabla \left(\delta \cdot \mathcal{A}_j(x,\sigma_j) \cdot \frac{\partial}{\partial \sigma_j} \phi_{1j}(x,\sigma_j) \right) d\sigma_j \\
&+ \sum_{j\in\mathcal{J}_z} \int_{\mathcal{J}_j^z} \frac{\partial}{\partial \sigma_j} \mathcal{B}_j(x,\sigma_j) \cdot \phi_{1j}(x,\sigma_j)\, d\sigma_j \\
&+ \sum_{j\in\mathcal{J}_z} \int_{\mathcal{J}_j^z} \Big(\mathcal{B}_j(x,\sigma_j) + \mathcal{C}_j(x,\sigma_j) \Big) \cdot \frac{\partial}{\partial \sigma_j} \phi_{1j}(x,\sigma_j)\, d\sigma_j \\
&- \sum_{j\in\mathcal{J}_z} \int_{\mathcal{J}_j^z} \gamma_j(\sigma_j) * \nabla \Big(\delta \cdot \mathcal{A}_j(x,\sigma_j) \cdot \gamma_j(\sigma_j) * \nabla \phi_0(x) \Big)\, d\sigma_j \\
&+ \sum_{j\in\mathcal{J}_z} \int_{\mathcal{J}_j^z} \gamma_j(\sigma_j) * \nabla \mathcal{B}_j(x,\sigma_j) \cdot \phi_0(x)\, d\sigma_j \\
&+ \sum_{j\in\mathcal{J}_z} \int_{\mathcal{J}_j^z} \Big(\mathcal{B}_j(x,\lambda_j) + \mathcal{C}_j(x,\sigma_j) \Big) \cdot \gamma_j(\sigma_j) * \nabla \phi_0(x)\, d\sigma_j \\
&+ \sum_{j\in\mathcal{J}_z} \int_{\mathcal{J}_j^z} \mathcal{D}_j(x,\sigma_j) \cdot \phi_0(x)\, d\sigma_j = \sum_{j\in\mathcal{J}_z} \int_{\mathcal{J}_j^z} \mathcal{F}_j(x,\sigma_j)\, d\sigma_j .
\end{aligned} \tag{10}
$$

The first six terms have the following representations:

- $$
\begin{aligned}
&\gamma_j(\sigma_j) * \nabla \left(\delta \cdot \mathcal{A}_j(x,\sigma_j) \cdot \frac{\partial}{\partial \sigma_j} \phi_{1j}(x,\sigma_j) \right) \\
&= \sum_{s=1}^{d} \gamma_j^{(s)}(\sigma_j) \cdot \frac{\partial}{\partial x_s} \Bigg(\delta \cdot \mathcal{A}_j(x,\sigma_j) \cdot \frac{\partial}{\partial \sigma_j} \Bigg(\sum_{k=1}^{d} \mathcal{S}_j^{(k)}(x,\sigma_j) \cdot \frac{\partial}{\partial x_k} \phi_0(x) \\
&- \mathcal{T}_j(x,\sigma_j) \cdot \phi_0(x) \Bigg) \Bigg) \\
&= \sum_{s=1}^{d} \sum_{k=1}^{d} \frac{\partial}{\partial x_s} \left(\gamma_j^{(s)}(\sigma_j) \cdot \delta \cdot \mathcal{A}_j(x,\sigma_j) \cdot \frac{\partial}{\partial \sigma_j} \mathcal{S}_j^{(k)}(x,\sigma_j) \cdot \frac{\partial}{\partial x_k} \phi_0(x) \right) \\
&- \sum_{s=1}^{d} \frac{\partial}{\partial x_s} \left(\gamma_j^{(s)}(\sigma_j) \cdot \delta \cdot \mathcal{A}_j(x,\sigma_j) \cdot \frac{\partial}{\partial \sigma_j} \mathcal{T}_j(x,\sigma_j) \cdot \phi_0(x) \right)
\end{aligned} \tag{11}
$$

- $$\frac{\partial}{\partial \sigma_j}\mathcal{B}_j(x,\sigma_j)\cdot\phi_{1j}(x,\sigma_j)$$
$$=\frac{\partial}{\partial \sigma_j}\mathcal{B}_j(x,\sigma_j)\cdot\left(\sum_{k=1}^{d}\mathcal{S}_j^{(k)}(x,\sigma_j)\cdot\frac{\partial}{\partial x_k}\phi_0(x)-\mathcal{T}_j(x,\sigma_j)\cdot\phi_0(x)\right)$$
$$=\sum_{k=1}^{d}\frac{\partial}{\partial \sigma_j}\mathcal{B}_j(x,\sigma_j)\cdot\mathcal{S}_j^{(k)}(x,\sigma_j)\cdot\frac{\partial}{\partial x_k}\phi_0(x)$$
$$-\ \frac{\partial}{\partial \sigma_j}\mathcal{B}_j(x,\sigma_j)\cdot\mathcal{T}_j(x,\sigma_j)\cdot\phi_0(x) \tag{12}$$

- $$\left(\mathcal{B}_j(x,\sigma_j)+\mathcal{C}_j(x,\sigma_j)\right)\cdot\frac{\partial}{\partial \sigma_j}\phi_{1j}(x,\sigma_j)$$
$$=\left(\mathcal{B}_j(x,\sigma_j)+\mathcal{C}_j(x,\sigma_j)\right)\cdot\frac{\partial}{\partial \sigma_j}\left(\sum_{k=1}^{d}\mathcal{S}_j^{(k)}(x,\sigma_j)\cdot\frac{\partial}{\partial x_k}\phi_0(x)\right.$$
$$\left.-\mathcal{T}_j(x,\sigma_j)\cdot\phi_0(x)\right)$$
$$=\sum_{k=1}^{d}\left(\mathcal{B}_j(x,\sigma_j)+\mathcal{C}_j(x,\sigma_j)\right)\cdot\frac{\partial}{\partial \sigma_j}\mathcal{S}_j^{(k)}(x,\sigma_j)\cdot\frac{\partial}{\partial x_k}\phi_0(x)$$
$$-\ \left(\mathcal{B}_j(x,\sigma_j)+\mathcal{C}_j(x,\sigma_j)\right)\cdot\frac{\partial}{\partial \sigma_j}\mathcal{T}_j(x,\sigma_j)\cdot\phi_0(x) \tag{13}$$

- $$w_j(\sigma_j)*\nabla\left(\delta\cdot\mathcal{A}_j(x,\sigma_j)\cdot\gamma_j(\sigma_j)*\nabla\phi_0(x)\right)$$
$$=\sum_{s=1}^{d}\gamma_j^{(s)}(\sigma_j)\cdot\frac{\partial}{\partial x_s}\left(\delta\cdot\mathcal{A}_j(x,\sigma_j)\cdot\sum_{k=1}^{d}\gamma_j^{(k)}(\sigma_j)\cdot\frac{\partial}{\partial x_k}\phi_0(x)\right)$$
$$=\sum_{s=1}^{d}\sum_{k=1}^{d}\frac{\partial}{\partial x_s}\left(\gamma_j^{(s)}(\sigma_j)\cdot\delta\cdot\mathcal{A}_j(x,\sigma_j)\cdot\gamma_j^{(k)}(\sigma_j)\cdot\frac{\partial}{\partial x_k}\phi_0(x)\right) \tag{14}$$

- $$\gamma_j(\sigma_j)*\nabla\mathcal{B}_j(x,\sigma_j)\cdot\phi_0(x)$$
$$=\sum_{s=1}^{d}\gamma_j^{(s)}(\sigma_j)\cdot\frac{\partial}{\partial x_s}\mathcal{B}_j(x,\sigma_j)\cdot\phi_0(x)$$
$$=\sum_{s=1}^{d}\frac{\partial}{\partial x_s}\left(\gamma_j^{(s)}(\sigma_j)\cdot\mathcal{B}_j(x,\sigma_j)\right)\cdot\phi_0(x) \tag{15}$$

$$
\begin{aligned}
\bullet\ & \Big(\mathcal{B}_j(x,\sigma_j)+\mathcal{C}_j(x,\sigma_j)\Big)\cdot\gamma_j(\sigma_j)*\nabla\phi_0(x)\\
&=\Big(\mathcal{B}_j(x,\sigma_j)+\mathcal{C}_j(x,\sigma_j)\Big)\cdot\sum_{k=1}^{d}\gamma_j^{(k)}(\sigma_j)\cdot\frac{\partial}{\partial x_k}\phi_0(x)\\
&=\sum_{k=1}^{d}\Big(\mathcal{B}_j(x,\sigma_j)+\mathcal{C}_j(x,\sigma_j)\Big)\cdot\gamma_j^{(k)}(\sigma_j)\cdot\frac{\partial}{\partial x_k}\phi_0(x). \qquad (16)
\end{aligned}
$$

By inserting (11)-(16) in (10) we obtain

$$
\begin{aligned}
&-\sum_{j\in\mathcal{J}_z}\int_{\mathcal{I}_j^z}\sum_{s=1}^{d}\sum_{k=1}^{d}\frac{\partial}{\partial x_s}\left(\delta\cdot\mathcal{A}_j(x,\sigma_j)\cdot\gamma_j^{(s)}(\sigma_j)\cdot\frac{\partial}{\partial\sigma_j}\mathcal{S}_j^{(k)}(x,\sigma_j)\cdot\frac{\partial}{\partial x_k}\phi_0(x)\right)d\sigma_j\\
&+\sum_{j\in\mathcal{J}_z}\int_{\mathcal{I}_j^z}\sum_{s=1}^{d}\frac{\partial}{\partial x_s}\left(\delta\cdot\mathcal{A}_j(x,\sigma_j)\cdot\gamma_j^{(s)}(\sigma_j)\cdot\frac{\partial}{\partial\sigma_j}\mathcal{T}_j(x,\sigma_j)\cdot\phi_0^{\delta}(x)\right)d\sigma_j\\
&+\sum_{j\in\mathcal{J}_z}\int_{\mathcal{I}_j^z}\sum_{k=1}^{d}\frac{\partial}{\partial\sigma_j}\mathcal{B}_j(x,\sigma_j)\cdot\mathcal{S}_j^{(k)}(x,\sigma_j)\cdot\frac{\partial}{\partial x_k}\phi_0(x)\,d\sigma_j\\
&-\sum_{j\in\mathcal{J}_z}\int_{\mathcal{I}_j^z}\frac{\partial}{\partial\sigma_j}\mathcal{B}_j(x,\sigma_j)\cdot\mathcal{T}_j(x,\sigma_j)\cdot\phi_0(x)\,d\sigma_j\\
&+\sum_{j\in\mathcal{J}_z}\int_{\mathcal{I}_j^z}\sum_{k=1}^{d}\Big(\mathcal{B}_j(x,\sigma_j)+\mathcal{C}_j(x,\sigma_j)\Big)\cdot\frac{\partial}{\partial\sigma_j}\mathcal{S}_j^{(k)}(x,\sigma_j)\cdot\frac{\partial}{\partial x_k}\phi_0(x)\,d\sigma_j\\
&-\sum_{j\in\mathcal{J}_z}\int_{\mathcal{I}_j^z}\Big(\mathcal{B}_j(x,\sigma_j)+\mathcal{C}_j(x,\sigma_j)\Big)\cdot\frac{\partial}{\partial\sigma_j}\mathcal{T}_j(x,\sigma_j)\cdot\phi_0(x)\,d\sigma_j\\
&-\sum_{j\in\mathcal{J}_z}\int_{\mathcal{I}_j^z}\sum_{s=1}^{d}\sum_{k=1}^{d}\frac{\partial}{\partial x_s}\left(\delta\cdot\mathcal{A}_j(x,\sigma_j)\cdot\gamma_j^{(s)}(\sigma_j)\cdot\gamma_j^{(k)}(\sigma_j)\cdot\frac{\partial}{\partial x_k}\phi_0(x)\right)d\sigma_j\\
&+\sum_{j\in\mathcal{J}_z}\int_{\mathcal{I}_j^z}\sum_{s=1}^{d}\frac{\partial}{\partial x_s}\Big(\gamma_j^{(s)}(\sigma_j)\cdot\mathcal{B}_j(x,\sigma_j)\Big)\cdot\phi_0(x)\,d\sigma_j\\
&+\sum_{j\in\mathcal{J}_z}\int_{\mathcal{I}_j^z}\sum_{k=1}^{d}\Big(\mathcal{B}_j(x,\sigma_j)+\mathcal{C}_j(x,\sigma_j)\Big)\cdot\gamma_j^{(k)}(\sigma_j)\cdot\frac{\partial}{\partial x_k}\phi_0(x)\,d\sigma_j\\
&+\sum_{j\in\mathcal{J}_z}\int_{\mathcal{I}_j^z}\mathcal{D}_j(x,\sigma_j)\cdot\phi_0(x)\,d\sigma_j=\sum_{j\in\mathcal{J}_z}\int_{\mathcal{I}_j^z}\mathcal{F}_j(x,\sigma_j)\,d\sigma_j.
\end{aligned}
$$

Then, after a further modification regarding $\mathcal{B}_j$ and $\mathcal{C}_j$, we get

$$
\begin{aligned}
&- \sum_{j\in\partial_z} \int_{\gamma_j^z} \sum_{s=1}^{d}\sum_{k=1}^{d} \frac{\partial}{\partial x_s}\left(\delta\cdot\mathcal{A}_j(x,\sigma_j)\cdot\gamma_j^{(s)}(\sigma_j)\cdot\frac{\partial}{\partial\sigma_j}\mathcal{S}_j^{(k)}(x,\sigma_j)\cdot\frac{\partial}{\partial x_k}\phi_0(x)\right)d\sigma_j\\
&- \sum_{j\in\partial_z} \int_{\gamma_j^z} \sum_{s=1}^{d}\sum_{k=1}^{d} \frac{\partial}{\partial x_s}\left(\delta\cdot\mathcal{A}_j(x,\sigma_j)\cdot\gamma_j^{(s)}(\sigma_j)\cdot\gamma_j^{(k)}(\sigma_j)\cdot\frac{\partial}{\partial x_k}\phi_0(x)\right)d\sigma_j\\
&+ \sum_{j\in\partial_z} \int_{\gamma_j^z} \sum_{s=1}^{d} \frac{\partial}{\partial x_s}\left(\delta\cdot\mathcal{A}_j(x,\sigma_j)\cdot\gamma_j^{(s)}(\sigma_j)\cdot\frac{\partial}{\partial\sigma_j}\mathcal{T}_j(x,\sigma_j)\cdot\phi_0(x)\right)d\sigma_j\\
&+ \sum_{j\in\partial_z} \int_{\gamma_j^z} \sum_{s=1}^{d} \frac{\partial}{\partial x_s}\left(\mathcal{B}_j(x,\sigma_j)\cdot\gamma_j^{(s)}(\sigma_j)\cdot\phi_0(x)\right)d\sigma_j\\
&+ \sum_{j\in\partial_z} \int_{\gamma_j^z} \sum_{s=1}^{d} \mathcal{C}_j(x,\sigma_j)\cdot\gamma_j^{(s)}(\sigma_j)\cdot\frac{\partial}{\partial x_s}\phi_0(x)\,d\sigma_j\\
&+ \sum_{j\in\partial_z} \int_{\gamma_j^z} \sum_{s=1}^{d} \frac{\partial}{\partial\sigma_j}\left(\mathcal{B}_j(x,\sigma_j)\cdot\mathcal{S}_j^{(s)}(x,\sigma_j)\right)\cdot\frac{\partial}{\partial x_s}\phi_0(x)\,d\sigma_j\\
&+ \sum_{j\in\partial_z} \int_{\gamma_j^z} \sum_{s=1}^{d} \mathcal{C}_j(x,\sigma_j)\cdot\frac{\partial}{\partial\sigma_j}\mathcal{S}_j^{(s)}(x,\sigma_j)\cdot\frac{\partial}{\partial x_s}\phi_0(x)\,d\sigma_j\\
&- \sum_{j\in\partial_z} \int_{\gamma_j^z} \mathcal{C}_j(x,\sigma_j)\cdot\frac{\partial}{\partial\sigma_j}\mathcal{T}_j(x,\sigma_j)\cdot\phi_0(x)\,d\sigma_j\\
&- \sum_{j\in\partial_z} \int_{\gamma_j^z} \frac{\partial}{\partial\sigma_j}\left(\mathcal{B}_j(x,\sigma_j)\cdot\mathcal{T}_j(x,\sigma_j)\right)\cdot\phi_0(x)\,d\sigma_j\\
&+ \sum_{j\in\partial_z} \int_{\gamma_j^z} \mathcal{D}_j(x,\sigma_j)\cdot\phi_0(x)\,d\sigma_j = \sum_{j\in\partial_z} \int_{\gamma_j^z} \mathcal{F}_j(x,\sigma_j)\,d\sigma_j.
\end{aligned}
$$

It follows immediately

$$
\begin{aligned}
&-\sum_{s=1}^{d}\sum_{k=1}^{d} \frac{\partial}{\partial x_s}\Bigg(\Bigg(\sum_{j\in\partial_z} \int_{\gamma_j^z} \delta\cdot\mathcal{A}_j(x,\sigma_j)\cdot\gamma_j^{(s)}(\sigma_j)\cdot\gamma_j^{(k)}(\sigma_j)\\
&+\delta\cdot\mathcal{A}_j(x,\sigma_j)\cdot\gamma_j^{(s)}(\sigma_j)\cdot\frac{\partial}{\partial\sigma_j}\mathcal{S}_j^{(k)}(x,\sigma_j)\,d\sigma_j\Bigg)\cdot\frac{\partial}{\partial x_k}\phi_0(x)\Bigg)\\
&+\sum_{s=1}^{d} \frac{\partial}{\partial x_s}\Bigg(\Bigg(\sum_{j\in\partial_z} \int_{\gamma_j^z} \mathcal{B}_j(x,\sigma_j)\cdot\gamma_j^{(s)}(\sigma_j)\\
&+\delta\cdot\mathcal{A}_j(x,\sigma_j)\cdot\gamma_j^{(s)}(\sigma_j)\cdot\frac{\partial}{\partial\sigma_j}\mathcal{T}_j(x,\sigma_j)\,d\sigma_j\Bigg)\cdot\phi_0(x)\Bigg)
\end{aligned}
$$

$$+\sum_{s=1}^{d}\Bigg(\sum_{j\in\partial_z}\int_{\gamma_j^z}\mathcal{C}_j(x,\sigma_j)\cdot\gamma_j^{(s)}(\sigma_j)+\mathcal{C}_j(x,\sigma_j)\cdot\frac{\partial}{\partial\sigma_j}\mathcal{S}_j^{(s)}(x,\sigma_j)$$
$$+\frac{\partial}{\partial\sigma_j}\Big(\mathcal{B}_j(x,\sigma_j)\cdot\mathcal{S}_j^{(s)}(x,\sigma_j)\Big)\,d\sigma_j\Bigg)\cdot\frac{\partial}{\partial x_k}\phi_0(x)$$
$$+\sum_{j\in\partial_z}\int_{\gamma_j^z}\Big(\mathcal{D}_j(x,\sigma_j)-\mathcal{C}_j(x,\sigma_j)\cdot\frac{\partial}{\partial\sigma_j}\phi_j(x,\sigma_j)$$
$$-\frac{\partial}{\partial\sigma_j}\Big(\mathcal{B}_j(x,\sigma_j)\cdot\mathcal{T}_j(x,\sigma_j)\Big)\Big)\,d\sigma_j\cdot\phi_0(x)=\sum_{j\in\partial_z}\int_{\gamma_j^z}\mathcal{F}_j(x,\sigma_j)\,d\sigma_j.$$

Finally, with the homogenized coefficients $\widehat{\mathcal{A}},\widehat{\mathcal{B}},\widehat{\mathcal{C}},\widehat{\mathcal{D}},\widehat{\mathcal{F}}$ and homogeneous Dirichlet boundary conditions we obtain the homogenized model.

$$\left.\begin{aligned}\mathcal{L}^0\phi_0(x)&=\widehat{\mathcal{F}}(x),\quad x\in\Omega,\\ \phi_0(x)&=0\qquad,\quad x\in\partial\Omega.\end{aligned}\right\}\ (\mathrm{MP}_0)$$

□

With the *homogenization process* described above, a macroscopic model (MP_0) is derived from the original microscopic model (MP_ε) by representing the solution of the microscopic model in terms of the two-scale asymptotic expansion (A). The original model on a ε-periodic network is replaced by an approximative model in terms of a singularly perturbed second-order partial differential equation on the full domain Ω. The homogenized model can be solved by standard software packages for partial differential equations of second order. The coefficients of the homogenized model characterize the effective behaviour of the microscopic model on a global scale (cf. Fig. 9).

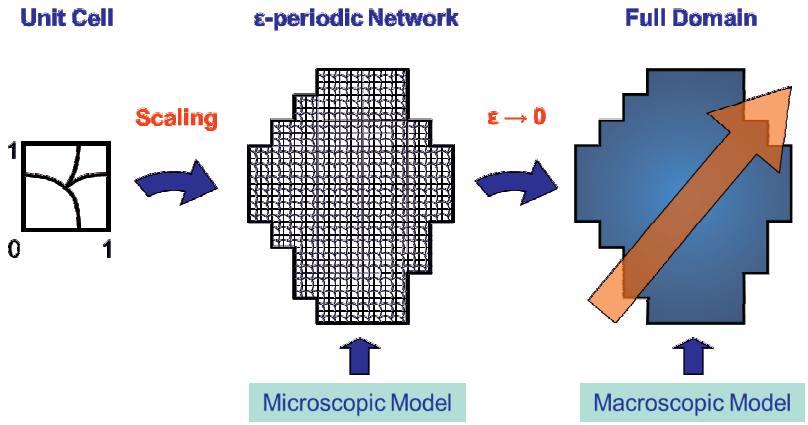

FIGURE 9. The homogenization process.

Each homogenized coefficient is obtained by averaging along the branches of the reference graph. In this way, the *micro-oscillations* of the microscopic model (as discussed in Section 1) are integrated into the macroscopic model, but in a smooth fashion. The homogenized coefficient $\widehat{\mathcal{B}}$ depends on the diffusion coefficient $\delta\mathcal{A}_j$. This influence is weak for advection-dominant microscopic models, where δ tends to zero. We further note, that the homogenized coefficient $\widehat{\mathcal{D}}$ depends on $\mathcal{B}_j$ and $\mathcal{C}_j$. The geometric structure of the periodic network that is represented by the topology of the reference graph directly affects the homogenized coefficients $\widehat{\mathcal{A}}_{sk}$, $\widehat{\mathcal{B}}_k$, $\widehat{\mathcal{C}}_k$, because these parameters depend on $\gamma_j^{(k)}$. In other words, the structure and the geometry of the reference graph directly takes influence on the global behaviour of the system.

Error Estimate

Since ε is small compared to the total diameter of the full region Ω, the macroscopic model (MP_0) provides an approximation for the microscopic model (MP_ε) on the network $\mathcal{N}_\varepsilon^\Omega$. This could be easily proofed by an evaluation of error estimates. We consider the *first-order approximation*

$$\phi^\varepsilon(x) \sim \phi_0(x) + \varepsilon \cdot \phi_1\Big(x, \frac{x}{\varepsilon}\Big),$$

with $\phi_1 = \mathcal{S} \circ \nabla\phi_0 - \mathcal{T} \cdot \phi_0$. The *residuum* $\mathfrak{R}^\varepsilon := \phi^\varepsilon - \phi_0 - \varepsilon\phi_1$ compares the exact solution, ϕ^ε, of the microscopic model on the network and the first order approximation. The following error result is obtained after some straightforward calculations[3]:

$$\|\mathfrak{R}^\varepsilon\|_{H^1(\mathcal{N}_\varepsilon^\Omega)} \leq C \cdot \varepsilon^{\frac{1}{2}}.$$

This inequality shows, that the the difference between the exact solution of the microscopic model and the first-order approximation tends to zero for $\varepsilon \to 0$.

7. **Regular Topologies.** In some particular geometric situations, the homogenized coefficients can be represented in a simplified way. The reference graph is called *regular*, if it consists of paths that are all completely crossing the reference cell from one of its sides to the opposite side (see Fig. 10).

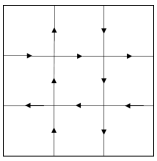

FIGURE 10. *Regular Topologies*: A regular reference graph.

[3]For further details we refer to [22], pages 122-152.

Because of the periodicity of $\mathcal{B}$, $\mathcal{S}^{(k)}$, and $\mathcal{T}$ the equations

$$\sum_{j\in\mathcal{J}^z}\int_{\mathcal{J}_j^z}\frac{\partial}{\partial\sigma_j}\Big(\mathcal{B}_j(x,\sigma_j)\cdot\mathcal{S}_j^{(k)}(x,\sigma_j)\Big)\,d\sigma_j=0$$

and

$$\sum_{j\in\mathcal{J}^y}\int_{\mathcal{J}_j^z}\frac{\partial}{\partial\sigma_j}\Big(\mathcal{B}_j(x,\sigma_j)\cdot\mathcal{T}_j(x,\sigma_j)\Big)\,d\sigma_j=0$$

are fulfilled for networks with regular reference graphs. With these equations the homogenized coefficients take the following simplified form:

$$\widehat{\mathcal{A}}_{sk}(x)=\sum_{j\in\mathcal{J}^z}\int_{\mathcal{J}_j^z}\delta\cdot\mathcal{A}_j(x,\sigma_j)\cdot\gamma_j^{(s)}(\sigma_j)\Big(\gamma_j^{(k)}(\sigma_j)+\frac{\partial}{\partial\sigma_j}\mathcal{S}_j^{(k)}(x,\sigma_j)\Big)\,d\sigma_j,$$

$$\widehat{\mathcal{B}}_k(x)$$

$$=\sum_{j\in\mathcal{J}^z}\int_{\mathcal{J}_j^z}\gamma_j^{(k)}(\sigma_j)\Big(\mathcal{B}_j(x,\sigma_j)+\delta\cdot\mathcal{A}_j(x,\sigma_j)\cdot\frac{\partial}{\partial\sigma_j}\mathcal{T}_j(x,\sigma_j)\Big)$$

$$\widehat{\mathcal{C}}_k(x)=\sum_{j\in\mathcal{J}^z}\int_{\mathcal{J}_j^z}\mathcal{C}_j(x,\sigma_j)\Big(\gamma_j^{(k)}(\sigma_j)+\frac{\partial}{\partial\sigma_j}\mathcal{S}_j^{(k)}(x,\sigma_j)\Big)\,d\sigma_j,$$

$$\widehat{\mathcal{D}}(x)=\sum_{j\in\mathcal{J}^z}\int_{\mathcal{J}_j^z}\mathcal{D}_j(x,\sigma_j)-\mathcal{C}_j(x,\sigma_j)\cdot\frac{\partial}{\partial\sigma_j}\mathcal{T}_j(x,\sigma_j)\,d\sigma_j,$$

$$\widehat{\mathcal{F}}(x)=\sum_{j\in\mathcal{J}^z}\int_{\mathcal{J}_j^z}\mathcal{F}_j(x,\sigma_j)\,d\sigma_j.$$

8. **Homogenization of Diffusion-Advection-Reaction Equations on 3D Grids.** In this section, we consider the example of a three dimensional network with the paraxial reference graph. By copying and scaling of the reference graph a three-dimensional network is created in the domain $\Omega=(0,10)^3$ (in Fig. 11, the length of periodicity is $\varepsilon=1$).

For a given length of periodicity $\varepsilon>0$ we consider the microscopic model (MP_ε) with Dirichlet boundary conditions. For sake of simplicity we assume that the coefficients $\mathcal{A},\mathcal{B},\mathcal{C},\mathcal{D}$ and the source term $\mathcal{F}$ of the microscopic model take constant values:

$$\left.\begin{aligned}-\delta\mathcal{A}\cdot\frac{d^2}{dl_j^2}\phi_j^\varepsilon(l_j)+(\mathcal{B}+\mathcal{C})\cdot\frac{d}{dl_j}\phi_j^\varepsilon(l_j)+\mathcal{D}\cdot\phi_j^\varepsilon(l_j)&=\mathcal{F},\ j\in\mathcal{J}_\varepsilon^\Omega,\ l_j\in\mathcal{I}_j^\varepsilon,\\ \phi^\varepsilon(\tau)&=0,\ \tau\in\partial^B(\mathcal{N}_\varepsilon^\Omega),\\ \mathcal{K}_\tau^{\Omega,\varepsilon}\Big(\delta\mathcal{A}\cdot\frac{d}{dl_j}\phi_j^\varepsilon\Big)&=0,\ \tau\in\partial^R(\mathcal{N}_\varepsilon^\Omega),\end{aligned}\right\}\tag{17}$$

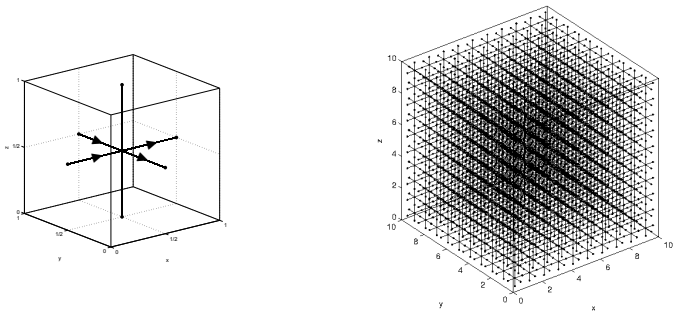

FIGURE 11. *Three-dimensional network*: The periodic network (right) is obtained by copying and scaling from the reference graph (left).

For each $j \in \mathcal{J}_\varepsilon^\Omega$ the exact solution of the microscopic model is given by

$$\phi_j^\varepsilon(l_j) = C_{1j} \cdot e^{\lambda_+ l_j} + C_{2j} \cdot e^{\lambda_- l_j} + \frac{\mathcal{F}}{\mathcal{D}}$$

with

$$\lambda_\pm = \frac{1}{2\delta\mathcal{A}} \cdot \left[\mathcal{B}+\mathcal{C} \pm \sqrt{(\mathcal{B}+\mathcal{C})^2 + 4\mathcal{D}\delta\mathcal{A}}\right]$$

The constant values $C_{1j}, C_{2j} \in \mathbb{R}$ are determined by the boundary conditions at the outer nodes of the network as well as the transmission conditions and continuity conditions at the ramification nodes. The homogenized coefficients are given by

$$\begin{aligned}
&\widehat{\mathcal{A}}_{11} = \widehat{\mathcal{A}}_{22} = \widehat{\mathcal{A}}_{33} = \delta\mathcal{A}, \quad \widehat{\mathcal{B}}_1 = -\widehat{\mathcal{B}}_2 = -\,\widehat{\mathcal{B}}_3 = \mathcal{B},\\
&\widehat{\mathcal{A}}_{12} = \widehat{\mathcal{A}}_{13} = \widehat{\mathcal{A}}_{21} = 0, \qquad \widehat{\mathcal{C}}_1 = -\widehat{\mathcal{C}}_2 = -\,\widehat{\mathcal{C}}_3 = \mathcal{C},\\
&\widehat{\mathcal{A}}_{31} = \widehat{\mathcal{A}}_{23} = \widehat{\mathcal{A}}_{32} = 0, \qquad \widehat{\mathcal{D}} = 3\mathcal{D},\ \widehat{\mathcal{F}} = 3\mathcal{F},
\end{aligned}$$

The corresponding macroscopic model takes the form

$$\left.\begin{aligned}
&-\delta\mathcal{A}\cdot\left[\frac{\partial^2}{\partial x_1^2}\phi_0(x) + \frac{\partial^2}{\partial x_2^2}\phi_0(x) + \frac{\partial^2}{\partial x_3^2}\phi_0(x)\right]\\
&+(\mathcal{B}+\mathcal{C})\cdot\left[\frac{\partial}{\partial x_1}\phi_0(x) - \frac{\partial}{\partial x_2}\phi_0(x) - \frac{\partial}{\partial x_3}\phi_0(x)\right]\\
&+3\mathcal{D}\cdot\phi_0(x) = 3\mathcal{F}, \quad x \in \Omega,\\
&\phi_0(x) = 0, \qquad x \in \partial\Omega.
\end{aligned}\right\}$$

The transport term of macroscopic model emphasizes the positive x_1-direction and the negative x_2 and x_3-directions and reflects in this way the topology of the reference graph.

In the next two subsections, we investigate the behaviour of the solution of (17) for two different parameter constellations. The first example illustrates the limit process of a diffusion-reaction-problem on an ε-periodic three-dimensional network with a symmetric solution. The second example focuses on the influence of the transport term and shows that the corresponding asymmetric solution of the diffusion-advection-reaction system converges towards the solution of the homogenized model on the full three-dimensional domain Ω.

8.1. **3D-Example: A Diffusion-Reaction Problem.** As a first example of the microscopic model we consider a diffusion-reaction-problem with the coefficients $\mathcal{A} = \mathcal{D} = \mathcal{F} = \delta = 1$ and $\mathcal{B} = \mathcal{C} = 0$. The microscopic model is given by

$$\left.\begin{aligned} -\frac{d^2}{dl_j^2}\phi_j^\varepsilon(l_j) + \phi_j^\varepsilon(l_j) &= 1,\ j \in \mathcal{J}_\varepsilon^\Omega,\ l_j \in \mathcal{I}_j^\varepsilon, \\ \phi^\varepsilon(\tau) &= 0,\ \tau \in \partial^B(\mathcal{N}_\varepsilon^\Omega), \\ \mathcal{K}_\tau^{\Omega,\varepsilon}\left(\frac{d}{dl_j}\phi_j^\varepsilon\right) &= 0,\ \tau \in \partial^R(\mathcal{N}_\varepsilon^\Omega), \end{aligned}\right\} \tag{18}$$

and the solution takes the form

$$\phi_j^\varepsilon(l_j) = C_{1j} \cdot e^{l_j} + C_{2j} \cdot e^{-l_j} + 1$$

on each edge $j \in \mathcal{J}_\varepsilon^\Omega$ with $l_j \in \mathcal{I}_j^\varepsilon$. The corresponding macroscopic model is

$$\left.\begin{aligned} -\frac{\partial^2}{\partial x_1^2}\phi_0(x) - \frac{\partial^2}{\partial x_2^2}\phi_0(x) - \frac{\partial^2}{\partial x_3^2}\phi_0(x) + 3 \cdot \phi_0(x) &= 3,\ x \in \Omega, \\ \phi_0(x) &= 0,\ x \in \partial\Omega. \end{aligned}\right\} \tag{19}$$

The following figures illustrate the behaviour of the solution of the microscopic model as well as the homogenized model in the 3D situation.

The solutions of these models take their values in the interval $[0, 1]$ and these values are represented with the colorbar in Fig. 12:

FIGURE 12. *Colorbar*: The solutions of the microscopic model and the homogenized model take their values in the interval $[0, 1]$.

Fig. 13 shows the exact solution of the network differential equation (18) for the different lengths of periodicity[4]. The figures on the right side show one half of the grid and on the left side slices in the middle of the x_1-x_2-direction.

The figures on the left side of Fig. 13 show that the solution u^ε is symmetric. This is because there is no transport term in (18). The corresponding homogenized solution u_0 of the macroscopic model (19) along the slice $E = \{(x, y, z) \in \overline{\Omega} \,|\, x = 5\}$ is depicted in Fig. 14. The solution u^ε of the microscopic model converges towards u_0 in the sense of two-scale approximation.

Fig. 15 shows the development of the solution of the network differential equation (18) for $\varepsilon \to 0$ in the inner part of the three-dimensional domain Ω. Here, the cube $W = [0, 5] \times [0, 5] \times [5, 10]$ is removed from the full domain Ω and it shows the part of the network $\mathcal{N}_\varepsilon^\Omega$ for $\varepsilon = 1$ and $\varepsilon = 0.5$ in $\overline{\Omega} \setminus W$.

[4]In each subfigure, the number of edges of the full network $\mathcal{N}_\varepsilon^\Omega$ and the corresponding length of periodicity ε are indicated in the form #edges/ε.

6000/1

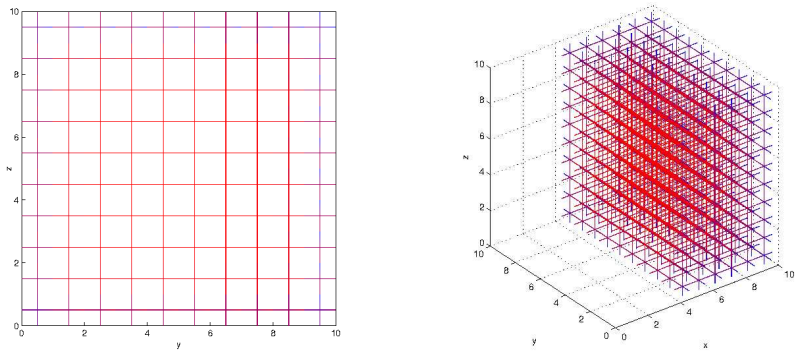

48000/0.5

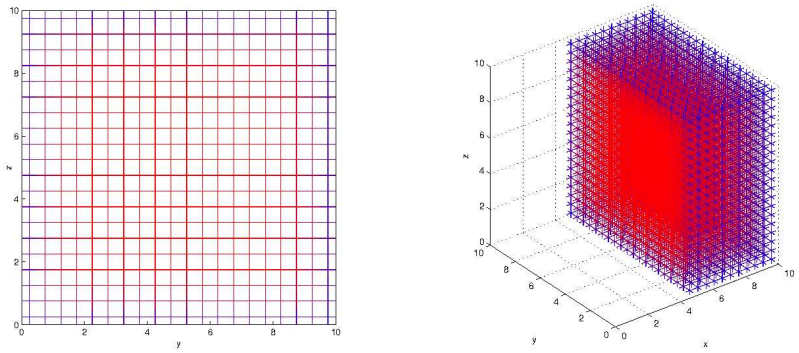

FIGURE 13. *3D-diffusion-reaction-problem*: Behaviour of the solution for $\varepsilon = 1$ and $\varepsilon = 0.5$.

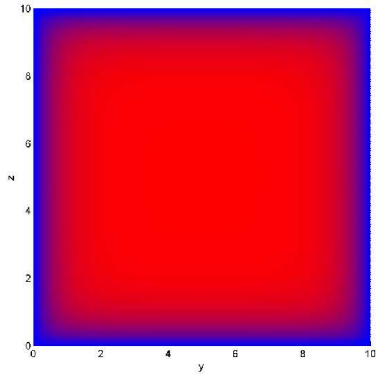

FIGURE 14. *Homogenized solution*: A slice through the cube.

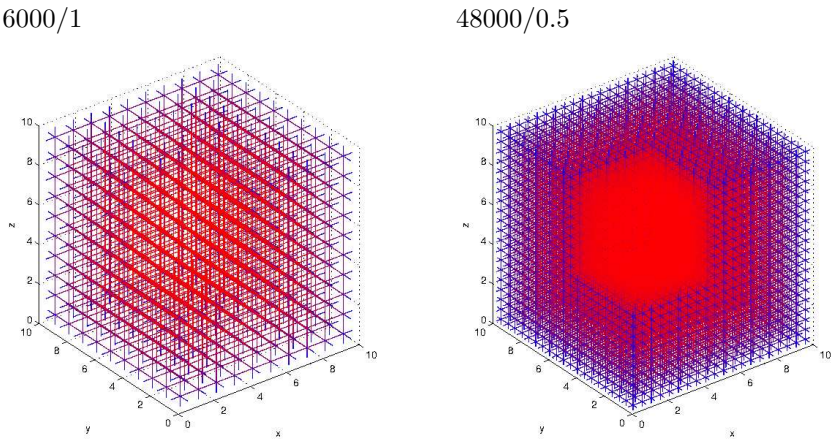

FIGURE 15. *3D-diffusion-reaction problem*: Behaviour of the solution.

It can be seen by Fig. 15 that the solution of the microscopic model converges towards the symmetric solution of the corresponding macroscopic model (19) in Fig. 16.

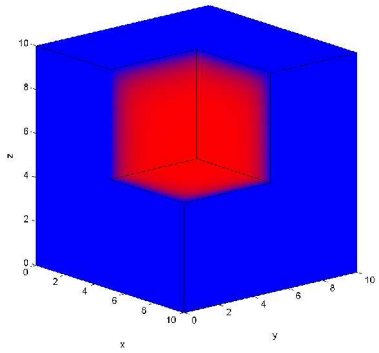

FIGURE 16. *Homogenized solution*: Inner part of the cube.

Table 1 shows the computational effort for the solution of the microscopic model (18) for various values of the scaling factor ε. We used an INTEL Core (TM) i3-3 110M CPU with 2.4 GHz and 4 GB primary memory. The corresponding homogenized model (19) can be solved in less than a second.

ε	#edges	#cells	time in sec.
1.0	6.000	1.000	2.3
$0.\overline{6}$	20.250	3.375	28.1
0.5	48.000	8.000	227.5
0.4	93.750	15.625	1039.9
$0.\overline{3}$	162.000	27.000	3395.2
0.29	257.250	42.875	9069.6
0.25	384.000	64.000	18897.1
$0.\overline{2}$	546.750	91.125	45392.3
0.2	750.000	125.000	80314.7

TABLE 1. *Computational effort*: Scaling factor ε, the number of edges, the number of cells and the computing time in seconds.

Fig. 17 displays the computation time in terms of the number of cells. Even in case of this very small cube with an edge length of ten units, the computation time increased drastically. The solution of the network differential equation for $\varepsilon = 0.2$ required more than twenty-two hours. In realistic models, for example filtering in oil recovery, huge capillary systems have to considered. A numerical solution of the corresponding microscopic models is completely unrealistic.

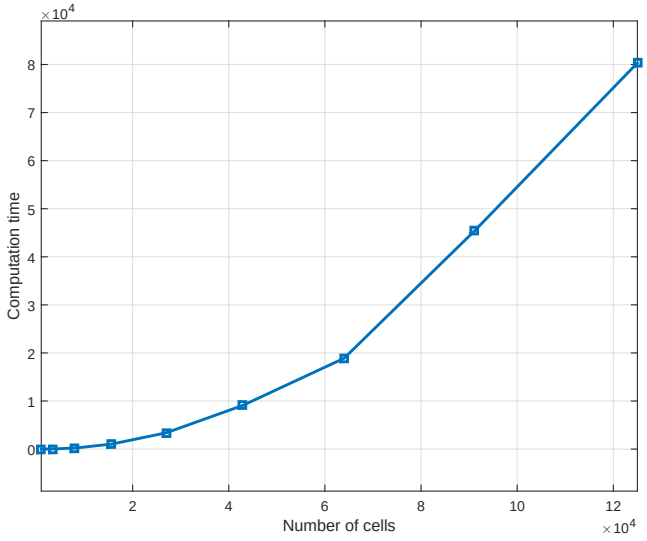

FIGURE 17. *Computation time*: Number of cells and the corresponding computation time.

9. **Reduced Equation.** In the formulation of the microscopic model (MP_ε) the parameter $\delta > 0$ is used to regulate the influence of the diffusion part of the system equation. If δ tends to zero, the microscopic model becomes *transport-dominated*. These types of problems usually require specialized numerical schemes in order to compensate the effects of *outflow boundaries*. In particular, for network differential equations such problems lead to numerical difficulties since the outflow boundaries arise *on each single edge*. Finite element solutions can show unexpected oscillations

near the outflow boundary, i.e., at the end of *each branch* of the network. For a numerical solution, the underlying discretization of the network requires a huge number of nodes and an extremely large algebraic system has to be solved. The paper [14] proposed a *mesh adaption technique* in a one-dimensional setting on a single edge for steady diffusion-convection-reaction equations. Other approaches include additional *stabilization terms* in the corresponding variational formulation [13]. The two-scale averaging technique discussed in this paper allows for an analysis of singularly perturbed microscopic models on periodic networks and, thus, *transport-dominant network differential equations*. Applying a formal asymptotic analysis $\delta \to 0$ with regard to the macroscopic model (MP_0), a so-called *reduced equation* is derived that can be easily solved with standard software packages:

$$\sum_{k=1}^{3} \frac{\partial}{\partial x_k}\left(\widehat{\mathcal{B}}_k^{red}(x)\cdot\phi_0(x)\right) + \sum_{k=1}^{3} \widehat{\mathcal{C}}_k^{red}(x)\cdot\frac{\partial}{\partial x_k}\phi_0(x) + \widehat{\mathcal{D}}^{red}(x)\cdot\phi_0(x) = \widehat{\mathcal{F}}^{red}(x).$$

The corresponding *reduced coefficients* take the form

$$\widehat{\mathcal{B}}_k^{red}(x) = \sum_{j\in\mathcal{J}^z}\int_{\mathcal{Y}_j^z} \mathcal{B}_j(x,\sigma_j)\cdot\gamma_j^{(k)}(\sigma_j)\,d\sigma_j,$$

$$\widehat{\mathcal{C}}_k^{red}(x) = \sum_{j\in\mathcal{J}^z}\int_{\mathcal{Y}_j^z} \mathcal{C}_j(x,\sigma_j)\cdot\gamma_j^{(k)}(\sigma_j) + \mathcal{C}_j(x,\sigma_j)\cdot\frac{\partial}{\partial\sigma_j}\mathcal{S}_j^{(k)}(x,\sigma_j) + \frac{\partial}{\partial\sigma_j}\left(\mathcal{B}_j(x,\sigma_j)\cdot\mathcal{S}_j^{(k)}(x,\sigma_j)\right)d\sigma_j,$$

$$\widehat{\mathcal{D}}^{red}(x) = \sum_{j\in\mathcal{J}^z}\int_{\mathcal{Y}_j^z} \mathcal{D}_j(x,\sigma_j) - \mathcal{C}_j(x,\sigma_j)\cdot\frac{\partial}{\partial\sigma_j}\mathcal{T}_j(x,\sigma_j) - \frac{\partial}{\partial\sigma_j}\left(\mathcal{B}_j(x,\sigma_j)\cdot\mathcal{T}_j(x,\sigma_j)\right)d\sigma_j,$$

$$\widehat{\mathcal{F}}^{red}(x) = \sum_{j\in\mathcal{J}^z}\int_{\mathcal{Y}_j^z} \mathcal{F}_j(x,\sigma_j)\,d\sigma_j.$$

Remark 2. We note that the reduced coefficients can be further simplified in case of networks with regular reference graphs that are defined by paths connecting border points on opposite sides of the reference cell. In such a situation, the reduced

coefficients are given by

$$\widehat{\mathcal{B}}_k^{red}(x) := \sum_{j\in\mathcal{J}^z} \int_{\mathcal{I}_j^z} \mathcal{B}_j(x,\sigma_j)\cdot\gamma_j^{(k)}(\sigma_j)\,d\sigma_j,$$

$$\widehat{\mathcal{C}}_k^{red}(x) := \sum_{j\in\mathcal{J}^z} \int_{\mathcal{I}_j^z} \mathcal{C}_j(x,\sigma_j)\cdot\gamma_j^{(k)}(\sigma_j) + \mathcal{C}_j(x,\sigma_j)\cdot\frac{\partial}{\partial\sigma_j}\mathcal{S}_j^{(k)}(x,\sigma_j)\,d\sigma_j,$$

$$\widehat{\mathcal{D}}^{red}(x) := \sum_{j\in\mathcal{J}^z} \int_{\mathcal{I}_j^z} \mathcal{D}_j(x,\sigma_j) - \mathcal{C}_j(x,\sigma_j)\cdot\frac{\partial}{\partial\sigma_j}\mathcal{T}_j(x,\sigma_j)\,d\sigma_j,$$

$$\widehat{\mathcal{F}}^{red}(x) := \sum_{j\in\mathcal{J}^z} \int_{\mathcal{I}_j^z} \mathcal{F}_j(x,\sigma_j)\,d\sigma_j.$$

10. **Numerical Example: A Transport-dominant Problem.** In this example, we consider a diffusion-advection-reaction problem on the network $\mathcal{N}_\varepsilon^\Omega$ with $\mathcal{A} = \mathcal{B} = \mathcal{C} = \mathcal{D} = \mathcal{F} = 1$ and $\delta = 0.01$. The corresponding microscopic model with Dirichlet boundary conditions has the form

$$\left.\begin{aligned} -0.01\cdot\frac{d^2}{dl_j^2}\phi_j^\varepsilon(l_j) + 2\cdot\frac{d}{dl_j}\phi_j^\varepsilon(l_j) + \phi_j^\varepsilon(l_j) &= 1, \quad j\in\mathcal{J}_\varepsilon^\Omega,\ l_j\in\mathcal{I}_j^\varepsilon,\\ \phi^\varepsilon(\tau) &= 0, \quad \tau\in\partial^B\mathcal{N}_\varepsilon^\Omega,\\ \mathcal{K}_\tau^{\Omega,\varepsilon}\left(0.01\cdot\frac{d}{dl_j}\phi_j^\varepsilon\right) &= 0, \quad \tau\in\partial^R\mathcal{N}_\varepsilon^\Omega. \end{aligned}\right\} \tag{20}$$

The solution is given by

$$\phi_j^\varepsilon(l_j) = C_{1j}\cdot e^{\frac{2+\sqrt{5}}{2}l_j} + C_{2j}\cdot e^{\frac{2-\sqrt{5}}{2}l_j} + 1.$$

The corresponding homogenized equation looks as follows

$$\left.\begin{aligned} -0.01\cdot\left[\tfrac{\partial^2}{\partial x_1^2}\phi_0(x) + \tfrac{\partial^2}{\partial x_2^2}\phi_0(x) + \tfrac{\partial^2}{\partial x_3^2}\phi_0(x)\right]&\\ +2\cdot\left[\tfrac{\partial}{\partial x_1}\phi_0(x) - \tfrac{\partial}{\partial x_2}\phi_0(x) - \tfrac{\partial}{\partial x_3}\phi_0(x)\right] + 3\cdot\phi_0(x) &= 3,\ x\in\Omega,\\ \phi_0(x) &= 0,\ x\in\partial\Omega. \end{aligned}\right\} \tag{21}$$

Now, we show the behaviour of the solution of the microscopic problem (20).

The figures in the left part of in Fig. 18 show slices along the middle of the network. The solution of the microscopic model is influenced by the transport term in the negative x_2- and x_3-directions. In addition, the solution ϕ^ε converges towards the solution ϕ_0 of the macroscopic model (21) for $\varepsilon\to 0$ as shown in the slice along the surface E in Fig. 19.

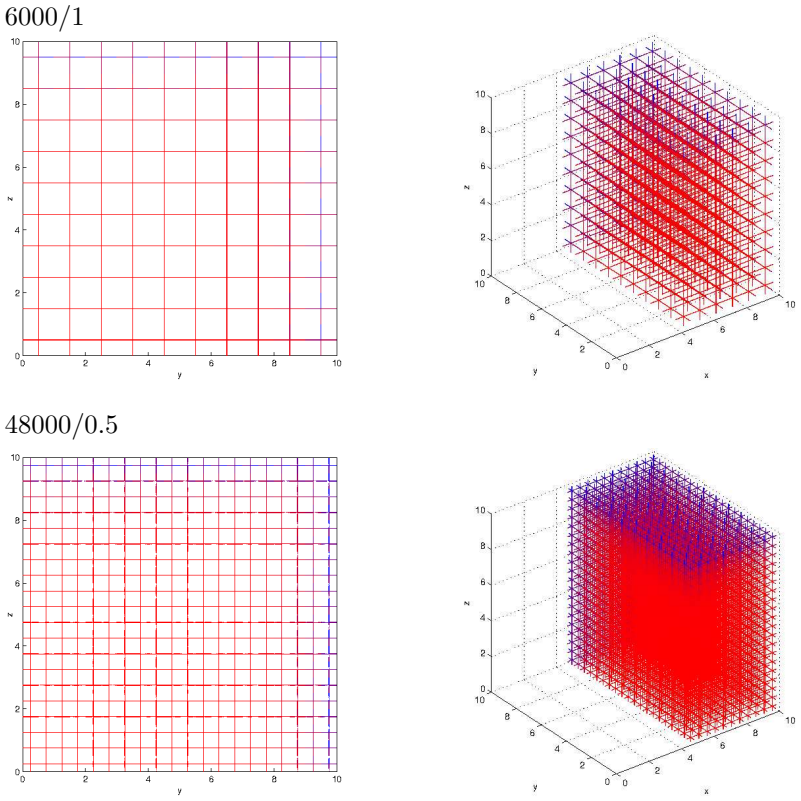

FIGURE 18. *3D-diffusion-advection-reaction-problem*: Behaviour of the solution.

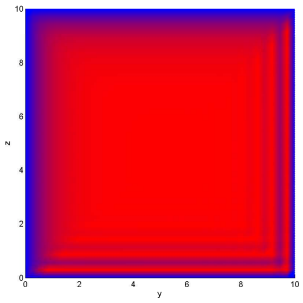

FIGURE 19. Slices along a surface: Homogenized solution.

Figs. 18-19 display the evolution of a boundary layer that reflects the structure of the reference graph. The boundary layer can also be recognized in the spatial slices depicted in Fig. 20.

Fig. 20 illustrates the behaviour of a singularly perturbed problem. It shows the solution of the macroscopic model along the surface $E = \{(x, y, z) \in \partial\Omega \,|\, y = 0\}$. Along the surface E, the solution $u^{\varepsilon,1}$ takes nearly the value 1 (red). In Fig. 21,

the solution of the corresponding macroscopic problem (i.e., the reduced problem) takes the value 0 (blue) because of the homogeneous boundary condition $u_0(x) = 0$ for *all* $x \in \partial\Omega$ of the Dirichlet boundary value problem.

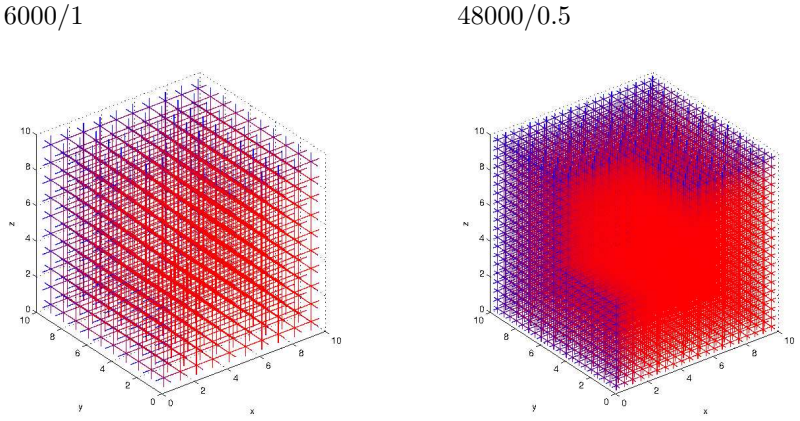

FIGURE 20. *Singularly perturbed 3D-diffusion-advection-reaction-problem*: Behaviour of the solution.

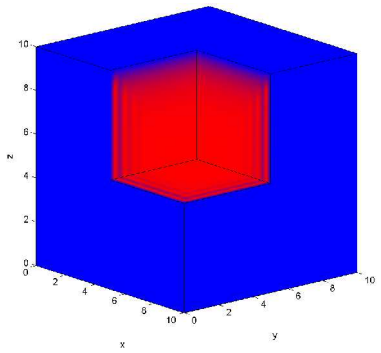

FIGURE 21. *Solution of the macroscopic model*: Inner part of the cube.

11. **Conclusion and Outlook.** Our studies in the field of OR-based models for *groundmotion prediction* and monitoring of *groundwater contamination* are often concerned with diffusion-advection-reaction problems on extremely large periodic capillary networks. The numerical solution of these problems is very challenging and easy-to-solve approximate models are strongly needed. The identification of the so-called homogenized models poses a research question on its own. Network differential equations are of significant importance in many applications ranging from engineering sciences and soil mechanics to nanotechnology and multi-scale physics. The numerical treatment of differential equations on extremely large networks is very challenging. In practical applications like flow problems in rock mechanics, the diameter of the region under consideration is very large when compared to the length of periodicity of the corresponding network structure. This results in a very high number of edges and huge number of intermediate nodes (or singularities), where

transmission conditions have to be fulfilled. In addition, the periodic microstructure of the network leads to highly oscillating coefficients that require a very fine discretization. A numerical solution of such problems is nearly impossible. The basic idea of this paper is to replace the difficult to solve microscopic model on the periodic network by an easy-to-solve approximating homogenized problem on the full domain. The proposed asymptotic analysis allows to derive the structure of the homogenized model and it reflects the effective behaviour of the microscopic model on a global scale. The corresponding homogenized coefficients describe the characteristics of network problem. They capture the effects of the micro-oscillations caused by the periodic structure of the network. In addition, they reflect the geometry of the network and the structure of the reference graph. This opens a perspective for future work, where the influence of the network topology on the macroscopic model and the effective behaviour could be addressed. In particular, such an approach could be used for topology optimization, for example for the development of network structures like bio-materials. Averaging strategies for optimal control problems on networks are a further promising direction of research. The asymptotic analysis of optimal control problems on periodic networks with a positive thickness of the branches is discussed in [18]. These approaches could be further extended to optimal control problems on graphs with a vanishing thickness of the edges. A completely new field of research are averaging strategies for stochastic systems on periodic networks. In future work, we intend to include the notion of almost periodicity in the sense of Bohr and Bochner into our analysis. The stochastic approaches offers a new perspective for applications in signal theory and for an investigation of the macroscopic behaviour of systems with microscopically periodic signals.

REFERENCES

[1] T. Arbogast, J. Douglas Jr. and U. Hornung, Derivation of the double porosity model of single phase flow via homogenization theory, *SIAM Journal on Mathematical Analysis*, **21** (1990), 823–836.

[2] J. L. Auriault and J. Lewandoska, Diffusion/adsorption/advection macrotransport in soils, *European Journal of Mechanics, A/Solids*, **15** (1996), 681–704.

[3] J. Bear, *Dynamics of Fluids in Porous Media*, Dover Publications, 1988.

[4] A. Bensoussan, J. L. Lions and G. Papanicolaou, *Asymptotic Analysis for Periodic Structures*, American Mathematical Society, Amsterdam, 2011.

[5] G. Bouchitté and I. Fragalà, Homogenization of elastic thin structures: a measure-fattening approach, *J. Convex Anal.*, **9** (2002), 1–24.

[6] C. Boutin, A. Rallu and S. Hans, Large scale modulation of high frequency acoustic waves in periodic porous media, *The Journal of the acoustical society of America*, **132** (2012), 3622–3636.

[7] E. Canon and M. Lenczner, Modelling of thin elastic plates with small piezoelectric inclusions and sistributed electronic circuits. Models for inclusions that are small with respect to the thickness of the plate, *Journal of Elasticity*, **55** (1999), 111–141.

[8] F. Civan, *Porous Media Transport Phenomena*, John Wiley & Sons, 2011.

[9] M. Cunha and L. Nunes, *Groundwater Characterization, Management and Monitoring*, WIT-Press, 2010.

[10] L. Dormieux and E. Lemarchand, Homogenization approach of advection and diffusion in cracked porous material, *Journal of Engineering Mechanics*, **127** (2001), 1267–1274.

[11] M. Espedal, A. Fasano and A. Mikelić, Filtration in porous media and industrial application, *Lecture Notes in Mathematics*, Lectures given at the 4th Session of the Centro Internazionale Matematico Estivo (C.I.M.E.) held in Cetraro, Italy August 24-29, 1998, **1734** (2000), Springer Berlin, Heidelberg.

[12] P. Exner, J. P. Keating, P. Kuchment, T. Sunada and A. Teplyaev, Analysis on Graphs and Its Applications - Proceedings of Symposia in Pure Mathematics, *American Mathematical Society*, **77** (2008).

[13] S. Franz and H.-G. Roos, *The capriciousness of numerical methods for singular perturbations*, *SIAM review*, **53** (2011), 157–173.
[14] A. Fortin, J. M. Urquiza and R. Bois, A mesh adaptation method for 1D-boundary layer problems, *International Journal of Numerical Analysis and Modeling, Series B*, **3** (2012), 408–428.
[15] S. Göktepe and C. Miehe, A micro-macro approach to rubber-like materials. Part III: The micro-sphere model of anisotropic Mullins-type damage, *Journal of the Mechanics and Physics of Solids*, **53** (2005), 2259–2283.
[16] U. Hornung, *Homogenization and Porous Media*, Springer, 1996.
[17] J. D. Joannopoulos, R. D. Meade and J. N. Winn, *Photonic Crystals*, Princeton University Press, Princeton, NJ, 2008.
[18] P. Kogut and G. Leugering, Asymptotic analysis of optimal control problems on periodic singular graphs, *Systems & Control: Foundations & Applications* Birkhäuser Boston, 2011.
[19] P. Kuchment, *Quantum graphs I: Some basic structures*, *Waves Random Media*, **14** (2004), 107–128.
[20] P. Kuchment, Quantum graphs: An introduction and a brief survey, in *Analysis on Graphs and Its Applications - Proceedings of Symposia in Pure Mathematics*(eds. P. Exner, J.P. Keating, P. Kuchment, T. Sunada and A. Teplyaev), American Mathematical Society, **77** (2008), 291–312.
[21] P. Kuchment and L. Kunyansky, Differential operators on graphs and photonic crystals, *Advances in Computational Mathematics*, **16** (2002), 263–290.
[22] E. Kropat, *Über die Homogenisierung von Netzwerk-Differentialgleichungen*, Wissenschaftlicher Verlag Berlin, Berlin, 2007.
[23] M. Lenczner, Multiscale model for atomic force microscope array mechanical behaviour, *Applied Physics Letters*, **90** (2007), ID: 091908.
[24] M. Lenczner and D. Mercier, Homogenization of periodic electrical networks including voltage to current amplifiers, *Multiscale Modeling and Simulation*, **2** (2004), 359–397.
[25] M. Lenczner and G. Senouci-Bereksi, Homogenization of electrical networks including voltage-to-voltage amplifiers, *Mathematical Models and Methods in Applied Sciences*, **9** (1999), 899–932.
[26] E. Marušić-Palokaa and S. Marušić, Computation of the permeability tensor for the fluid flow through a periodic net of thin channels, *Applicable Analysis*, **64** (1997), 27–37.
[27] V. G. Mazja, S. A. Nasarow and B. A. Plamenewski, *Asymptotische Theorie elliptischer Randwertaufgaben in Singulär gestörten Gebieten II*, Wiley, Berlin, 1991.
[28] C. Miehe and S. Göktepe, A micro-macro approach to rubber-like materials. Part II: The micro-sphere model of finite rubber viscoelasticity, *Journal of the Mechanics and Physics of Solids*, **53** (2005), 2231–2258.
[29] C. Miehe, S. Göktepe and F. Lulei, A micro-macro approach to rubber-like materials - Part I: the non-affine micro-sphere model of rubber elasticity, *Journal of the Mechanics and Physics of Solids*, **52** (2004), 2617–2660.
[30] C. O. Ng and C. C. Mei, Homogenization theory applied to soil vapor extraction in aggregated soils, *Physics of Fluids*, **8** (1996), 2298–2306.
[31] M. Vogelius, A homogenization result for planar, polygonal networks, *RAIRO Modélisation Mathématique et Analyse Numérique*, **25** (1991), 483–514.
[32] F. Yerlikaya-Özkurta, A. Askanb and G.-W. Weber, An alternative approach to the ground motion prediction problem by a non-parametric adaptive regression method, *Engineering Optimization*, **46** (2014), 1651–1668.

Received October 2015; 1^{st} revision June 2016; final revision July 2016.

E-mail address: Erik.Kropat@unibw.de
E-mail address: Silja.Meyer-Nieberg@unibw.de
E-mail address: gweber@metu.edu.tr